ASSESSMENT OF THE DIRECT GENERALIZED BLOCH APPROACH B0: APPLICATION TO THE Li AND Be ATOMS AND THE MOLECULES LiH, BeH, AND THE PHENOLATE ANION

Holger MEISSNER

Department of Applied Mathematics, University of Waterloo, Waterloo, Ontario, N2L 3G1 Canada; e-mail: holger.meissner@chemie.uni-regensburg.de

Received January 31, 2005
Accepted July 1, 2005

Dedicated to Professor Josef Paldus on the occasion of his 70th birthday.

Besides the necessity of the development of sophisticated methods to calculate correlation energies – be it the coupled-cluster (CC) or the configuration-interaction (CI) methods and their various approaches – one also accentuate the need for efficient and less demanding methods in the area of medium and large molecular systems. Therefore, this article proposes a computational efficient and in our opinion reasonable approach for the calculation of correlation energies for medium and even larger molecules. This approach, named B0, based on the so-called direct generalized Bloch (DGB) equation which has already been successfully applied to small systems. Within those considerations the B0 approach showed promising results so that further investigations are worthwhile. Here, as a further step in the assessment of this method we apply the B0 approach to the Li and Be atoms as well as the LiH and BeH molecules. Molecules which show open and closed shell characteristics in the equilibrium and in the case of dissociation as well. The results are compared with CC and CI and experimental results if available. Since this results are encouraging even when considering small basis sets and with the prospect of larger molecular systems, therefore, we perform also B0 energy calculations for the low-lying states of the phenolate anion which for instance can be used in a simple model of the photoactive yellow protein (PYP) chromophore.
Keywords: *Ab initio* calculations; Generalized Bloch equation; B0-based approaches; Spectroscopic constants; Dipole moments; LiH, BeH hydrides; Phenolate anion; Coupled cluster; Configuration interaction.

It cannot be denied that present day quantum chemistry relies, besides the theoretical progress, strongly on the computational progress, be it the development of algorithms or the development of hardware. The general requirement of today's computer-aided chemistry (CAC) is both the accurate and efficient calculation of physical and chemical quantities. That includes, above all, highly accurate energy calculations – that in turn require an ac-

curate determination of the electron-correlation energy – without an excessive computational effort. In general, this requirement is still far from being universally fulfilled. Nonetheless, the successes, especially of the *ab initio* methods, have been most remarkable in this regard, as amply documented by the computations of electronic properties of small and medium-sized molecules[1]. Here, the various single-reference coupled-cluster (CC) methods[2–5] or the various multireference (MR) methods[6–8] (for an overview, see, e.g., ref. 12 in ref.[9]) belong to the most accurate and widely used methods for the determination of the molecular electronic structure in the CAC.

However, despite the advantages of the CC ansatz, especially in its truncated version, i.e., when considering only the singly (S) and doubly (D) excited configurations relative to a single reference (SR) wave function (SR CCSD), or in the widely exploited CCSD(T) method that accounts perturbatively for triply (T) excited configurations, there are still certain inherent problems (see, e.g., ref.[10]) that limit the general applicability of these approaches. Especially if we are interested in properties of larger molecular systems which occur in biochemistry as, e.g., acid derivatives, which act as a chromophore in photoactive proteins, these methods suffer besides the inherent problems also from their complexity making high demands on the computational capacity and equipment.

Thus, it appears that one has to simplify sophisticated methods in order to reduce the computational effort. However, only so far that the main characteristic features of molecular systems can be covered by such method. To achieve these requirements we exploit the so-called B0 approach which is based on the direct generalized Bloch (DGB)[11] method. In the first place of this assessment of the B0 approach we apply this DGB approximation to the Li and Be atoms and afterwards to the LiH and BeH molecules so that we can compare the results with highly accurate CC and CI results and experimental results if available. In a next step with regard to larger molecular systems we apply the B0 approach to the phenolate anion. This is motivated by the fact that a phenolate anion surrounded by amino acids can be used as a simple model for the photoactive yellow protein (PYP) chromophore[12]. Where, the PYP is a small soluble protein found in a halophilic bacterium used therein as a light sensor. Therefore, studies of PYP are not only of theoretical interest, but also are useful to understand the behavior of other visual pigments, such as the rhodopsins.

The theoretical consideration of the DGB method and, especially, of the B0 approach is shown in Section I. Then, numerical considerations are discussed in Section II and results of various approximations are shown in Sec-

tion III. Finally, Section IV gives a summary on this alternative method and its variants.

I. THEORETICAL CONSIDERATION

Here, we present a brief summary of the direct iterative approach to the solution of the generalized Bloch equation (for more details we refer to ref.[11]).

The general MR approaches employ the concept of the *reference* space $\mathcal{M}_0$, representing a suitable, finite-dimensional subspace of the *N*-electron space $\mathcal{V}$ which is spanned by all possible *N*-electron configuration states (or Slater determinants) Φ_α. In all practical calculations, $\mathcal{V}$ is also finite-dimensional and is given by the choice of the atomic orbital (AO) basis set defining a given *ab initio* model. An *n*-dimensional (complete or incomplete) reference space $\mathcal{M}_0$ is defined as a linear span of *n* orthonormal configurations Φ_α, $\alpha \in I_\mathrm{p} \equiv \{1, \cdots, n\}$, the remaining configurations Φ_α, $\alpha \in I_\mathrm{q} \equiv \{n+1, \cdots, n+m\}$ defining its orthogonal complement $\mathcal{M}_0^\perp$ in $\mathcal{V}$. The orthogonal projectors onto $\mathcal{M}_0$ and $\mathcal{M}_0^\perp$ are then designated by $\hat{P}$ and $\hat{Q}$, respectively, so that $\hat{P} + \hat{Q} = \hat{1}$, the identity operator on $\mathcal{V} = \mathcal{M}_0 \oplus \mathcal{M}_0^\perp$.

The basic assumption of any MR approach is that with a suitably chosen set of *n* exact *N*-electron eigenstates Ψ_a ($a \in I_\mathrm{p}$) of a given Hamiltonian $\hat{H}$,

$$\hat{H}\Psi_a = E_a \Psi_a \,, \quad a \in I_\mathrm{p} \,, \tag{1}$$

referred to as the *target states*, we can associate an *n*-dimensional reference space $\mathcal{M}_0$ providing a reasonable zero-order approximation for Ψ_a in a sense that their projections onto $\mathcal{M}_0$, $\hat{P}\Psi_a = \Psi_a^{(0)}$, $a \in I_\mathrm{p}$, span $\mathcal{M}_0$, so that

$$\mathcal{M}_0 = \mathrm{span}\,\{\Psi_a^{(0)} | a \in I_\mathrm{p}\} = \mathrm{span}\,\{\Phi_\alpha | \alpha \in I_\mathrm{p}\}\,. \tag{2}$$

Here E_a ($a \in I_\mathrm{p}$) designate the corresponding exact eigenvalues of $\hat{H}$, and the *n*-dimensional space $\mathcal{M} = \mathrm{span}\,\{\Psi_a | a \in I_\mathrm{p}\}$ is referred to as the *target space*. In the intermediate normalization,

$$\langle \Psi_a^{(0)} | \Psi_a \rangle = \langle \Psi_a^{(0)} | \Psi_a^{(0)} \rangle = 1 \,, \quad a \in I_\mathrm{p} \,, \tag{3}$$

the target states Ψ_a ($a \in I_p$) may be represented as follows

$$\Psi_a = \Psi_a^{(0)} + \Psi_a^{(\perp)} = \sum_{\alpha \in I_p} g_\alpha^a \Phi_\alpha + \sum_{\lambda \in I_q} c_\lambda^a \Phi_\lambda \ . \tag{4}$$

With this formulation, the main task is to set up the equations of motion that enable us to determine the energies E_a as well as the coefficients $g_\alpha^a = \langle \Phi_\alpha | \Psi_a \rangle$, $(a, \alpha \in I_p)$, and the wave function expansion coefficients (WECs) $c_\lambda^a = \langle \Phi_\lambda | \Psi_a \rangle$, $(a \in I_p, \lambda \in I_q)$, defining the reference space component $\Psi_a^{(0)}$ and the outer space component $\Psi_a^{\perp}$ of Ψ_a, respectively.

In order to determine the outer part of Ψ_a that is responsible for the dynamic correlation, we rely on the generalized Bloch equation $\hat{U}\hat{H}\hat{U}\Psi_a^{(0)} = \hat{H}\hat{U}\Psi_a^{(0)}$, which is obtained by acting with the so-called wave-operator $\hat{U}$ on the Schrödinger equation (*1*) (for details, see ref.[11]). This equation then determines the *outer space* coefficients

$$c_\lambda^a = \langle \Phi_\lambda | \hat{U} | \Psi_a \rangle = \langle \Phi_\lambda | \hat{U} | \Psi_a^{(0)} \rangle, \quad a \in I_p \ , \lambda \in I_q \ , \tag{5}$$

as well as an effective Hamiltonian $\hat{H}^{(\mathrm{eff})}$ to determine the g_α^a coefficients (see ref.[11]). In matrix form, the Bloch equation can be represented as follows

$$\langle \mathbf{\Phi}_q | (1 - \hat{U}) \hat{H} \hat{U} | \mathbf{\Psi}^{(0)} \rangle = 0 \tag{6}$$

while the energies are given by

$$\mathbf{E} = \langle \tilde{\mathbf{\Psi}}^{(0)} | \hat{H} \hat{U} | \mathbf{\Psi}^{(0)} \rangle \tag{7}$$

where $\tilde{\mathbf{\Psi}}^{(0)}$ represents the corresponding dual basis of $\mathbf{\Psi}^{(0)}$. These two equations, Eqs (*6*) and (*7*), thus represent the basic formulas for the determination of the explicit representation of the equation for the *outer space* coefficients:

$$H_{\tilde{a}\lambda} (c_\lambda^a)^2 - \Lambda_{\lambda a} c_\lambda^a - (H_{\lambda a} + \Gamma_{\lambda a}) = 0 \tag{8}$$

where

$$\Lambda_{\lambda a} = H_{\lambda\lambda} - H_{\tilde{a}a} - \sum_{\mu \in I_q \setminus \lambda} H_{\tilde{a}\mu} c_\mu^a - \sum_{b \in I_p \setminus a} H_{\tilde{b}\lambda} c_\lambda^b \qquad (9a)$$

$$\Gamma_{\lambda a} = \sum_{\mu \in I_q \setminus \lambda} H_{\lambda\mu} c_\mu^a - \sum_{b \in I_p \setminus a} H_{\tilde{b}a} c_\lambda^b - \sum_{\substack{b \in I_p \setminus a \\ \mu \in I_q \setminus \lambda}} c_\lambda^b H_{\tilde{b}\mu} c_\mu^a \,. \qquad (9b)$$

Solving Eq. (*8*) for c_λ^a, we obtain

$$c_\lambda^a = \tfrac{1}{2}\{\Lambda_{\lambda a} - \sigma_\lambda^a [(\Lambda_{\lambda a})^2 + 4H_{\tilde{a}\lambda}(H_{\lambda a} + \Gamma_{\lambda a})]^{1/2}\} / H_{\tilde{a}\lambda} \,, \quad \sigma_\lambda^a = \mathrm{sgn}(\Lambda_{\lambda a}) \,, \quad (10)$$

which leads directly to an iterative scheme (e.g., by using the Jacobi–Newton algorithm). Here, i.e. $H_{\lambda\mu}$ stands for the matrix element of the Hamiltonian $\hat{H}$ and the functions labeled by λ and μ, respectively.

As in our former calculations[11] we exploit here the *state-selective* or *state-specific* (SS) version of the DGB formalism, by focusing on one state at a time. In terms of the general MR formalism this implies that we only require the zero-order approximation in the iterative scheme for the effective Hamiltonian. Thus, to obtain suitable reference states, we first diagonalize the Hamiltonian within the model space $\mathcal{M}_0$, obtaining the zero-order eigenstates $|\overline{\Psi}_a^{(0)}\rangle$,

$$|\overline{\Psi}_a^{(0)}\rangle = \sum_{\alpha \in I_p} q_a^{(\alpha)} |\Phi_\alpha\rangle \,, \quad \langle \overline{\Psi}_a^{(0)} | \overline{\Psi}_b^{(0)} \rangle = \delta_{ab} \,, \quad a, b \in I_p \,, \qquad (11)$$

and the corresponding eigenvalues $\overline{E}_a^{(0)} = \langle \overline{\Psi}_a^{(0)} | \hat{H} | \overline{\Psi}_a^{(0)} \rangle$. We then partition $\mathcal{M}_0$ into a one-dimensional reference $\mathcal{M}_0^{(a)}$, $\mathcal{M}_0^{(a)} = \mathrm{span}\{|\overline{\Psi}_a^{(0)}\rangle\}$ corresponding to $|\overline{\Psi}_a^{(0)}\rangle$, and the associated residual reference space $\mathcal{R}_0^{(a)}$, $\mathcal{R}_0^{(a)} = \mathrm{span}\{|\overline{\Psi}_b^{(0)}\rangle \,|\, b \in I_p \setminus \{a\}\}$, as follows

$$|\overline{\Psi}_a\rangle = |\overline{\Psi}_a^{(0)}\rangle + \sum_{\substack{b \in I_p \\ (b \neq a)}} \bar{c}_b^a |\overline{\Psi}_b^{(0)}\rangle + \sum_{\lambda \in I_q} \bar{c}_\lambda^a |\Phi_\lambda\rangle \,. \qquad (12)$$

Eventually, $|\overline{\Psi}_a\rangle$ represents the same state as $|\Psi_a\rangle$ except for the normalization and, likewise, $\bar{c}_\lambda^a$ represent renormalized coefficients c_λ^a of Eq. (*10*). The coefficients $\bar{c}_b^a$, associated with $\mathcal{R}_0^{(a)}$, should play only a secondary role, so

that $||\bar{c}_b^a|| << 1, \forall b \in I_p \setminus \{a\}$, since the static, and most of the non-dynamic, correlation effects should be already accounted for in $|\overline{\Psi}_a^{(0)}\rangle$, i.e. in $\mathcal{M}_0^{(a)}$, so that $\mathcal{M}_0^{(\perp)}$ will be responsible primarily for the dynamic correlation.

II. NUMERICAL CONSIDERATION

A. Computational Details

Of course, the structure of the SS reference space $\mathcal{M}_0^{(a)}$, and of the residual space $\mathcal{R}_0^{(a)}$, crucially depends on the *N*-electron configuration state functions (CSFs) $|\Phi_\lambda\rangle$ that are employed. For these CSFs we employ the $\hat{S}_z$-adapted Slater determinants or, respectively, linear combinations of Slater determinants which represent symmetry-adapted states. We refer to such a formalism as the SS single configuration (SC) approach and, in particular, since our current codes allow only to handle reference configurations consisting of at most two determinants, as the 1D or 2D SS approach.

Here, the 1D SS-SC approach can be applied, e.g. to the closed-shell ground states and the high-spin open-shell states, while in particular the 2D approach is necessary for the singlet excited state. In view of our earlier results, we primarily exploit the B0, BD_2, BQ_2, and BQe_2 approximations, with the emphasis on B0 (for more details of the various DGB approaches we refer to the ref.[11] especially, cf. d) of ref.[11]). We recall that in the 1D or closed-shell case, the BD_2 and BQe_2 approximations are equivalent to the standard SR CISD and CCSD approaches, respectively. The B0 approach is the simplest and therefore computationally most efficient approach in the hierarchy of the DGB methods, since it relies only on singly and doubly excited WECs where the $\Gamma_{\lambda a}$ parts of Eq. (*10*) are neglected. It is therefore worthwhile to assess the reliability of the B0 approach for the determination of the spectroscopic quantities, since it can be easily exploited even for rather large systems.

Moreover, we will here exploit a kind of internal correction in order to improve the B0 approximation on a low level of computational cost. A basic step in each calculation of the correlation energy is a single iteration step in which each WEC is recalculated by Eq. (*10*). Now, the internal correction is based on this $\Gamma_{\lambda a}$ term (neglected in B0). At a certain step of iteration we take into account these terms at a higher level of DGB approaches like e.g. BD_2 or BQe_2 just for one iteration step. In the rest of the B0 iteration this terms will be kept frozen. This leads in principle to a plethora of various internal corrections, here designated as B0[app], where app stands for the internal DGB approach used. Thus, an internal correction based on

BD_2 is called B0[D_2]. Besides the kind of level (app) of internal correction the question arises at which step this correction has to be incorporated. In our investigations the best results occur at a difference of successive correlation energies of 10^{-5}: $|E(i) - E(i-1)| \approx 10^{-5}$ which is here used for the calculation of the internal corrections. Of course, this modus operandi can also be applied at the end of the iteration, which has been already successfully utilized in former calculations[11]. It means we perform an additional iteration step with the obtained B0 coefficient but at a higher level of approximation of the WECs included in the $\Gamma_{\lambda a}$ terms. In the following the notation of these approaches is given as B0[app_1, app_2] where app_1 belongs to the internal correction of the B0 coefficients whereas the second term app_2 represents the kind of the additional iteration step at the end in our approximation scheme. If only one of these types of approaches is applied, the other one will be represented as dash, i.e., e.g., for the BD_2 internal correction we have B0[D_2,–] and vice versa. Here, it should also be mentioned that to simplify matters we will discard the 'B' in the label of the DGB approaches for labels of app. Of course, this procedure is not invariably assigned to B0 but also to other approaches of the DGB method. At that point it should be stressed that besides the internal corrections one can also use external coefficients in the calculations of the $\Gamma_{\lambda a}$ terms for the WECs of higher excitation than singly and doubly excited determinants. In this context, however, we have to search for a source of coefficients which is efficiently accessible, especially with regard to its computational demanding. For the application of external corrections in connection with the CCSD method, we refer to the refs[4,8,14–16].

Beside these internal corrections we also investigate the so-called size-extensivity corrections added on top of the DGB calculations. These corrections are originally designed for the CISD approximation to correct the size-extensivity shortcoming of truncated CI methods. Here, we will apply the following corrections, labeled by the initials of the name who introduced these corrections (cf. also ref.[17]):

1. Davidson[18,19] $: E_{dc} = E_{corr}(1 - C_o^2)$ (*13*)

2. Renormalized E_{dc}[20] $: E_{rdc} = \dfrac{E_{dc}}{C_o^2}$ (*14*)

3. Davidson–Silver[21] $: E_{dsc} = \dfrac{E_{dc}}{2C_o^2 - 1}$ (*15*)

4. Pople[22] $$: E_{\mathrm{pc}} = E_{\mathrm{corr}} \frac{\sqrt{n_{\mathrm{o}}(n_{\mathrm{o}} + 2\tan^2(2t))} - n_{\mathrm{o}}}{2(\sec(2t) - 1) - 1} \qquad (16)$$

5. Duch–Diercksen[23] $$: E_{\mathrm{ddc}} = \frac{E_{\mathrm{dc}}}{2((n_{\mathrm{o}} - 1)/(n_{\mathrm{o}} - 2))C_{\mathrm{o}}^2 - 1} \qquad (17)$$

6. Meissner[24] $$: E_{\mathrm{mc}} = E_{\mathrm{rdc}} \frac{(n_{\mathrm{o}} - 2)(n_{\mathrm{o}} - 3)}{n_{\mathrm{o}}(n_{\mathrm{o}} - 1)} \qquad (18)$$

7. Molnar–Szalay[25] $$: E_{\mathrm{msc}} = E_{\mathrm{dc}} \frac{(n_{\mathrm{o}} - 2)(n_{\mathrm{o}} - 3)(n_{\mathrm{v}} - 2)(n_{\mathrm{v}} - 3)}{n_{\mathrm{o}}(n_{\mathrm{o}} - 1)\, n_{\mathrm{v}}(n_{\mathrm{v}} - 1)} \qquad (19)$$

where E_{corr} is the correlation energy, n_{o} is the number of active electrons, n_{v} is the number of active (vacant or unoccupied) spin-orbitals, and t is derived from $\cos(t) = C_{\mathrm{o}}$ with C_{o} the renormalized coefficient of the reference wave function of the DGB approach applied. As we can see the Duch–Diercksen correction (E_{ddc}, Eq. (*17*) is a modification of the Davidson–Silver correction (E_{dsc}, Eq. (*15*)), which also holds for the Pople correction (E_{pc}, Eq. (*16*)). Furthermore, Eq. (*18*) and Eq. (*19*) are almost equivalent if the renormalized and the original Davidson correction hardly differ from each other in the case that we exploit a large basis set. Then the last part of the Molnar–Szalay correction, which takes into account the finiteness of a numerical basis set by the number of active orbitals, n_{v}, approaches the value one. On the other hand, if we take a look at the first three corrections, they should not differ from each other if the reference function represents the main contribution to the state of consideration. This means the coefficient C_{o} is of the magnitude ≈ 1 so that these approaches are almost equivalent. Thus, at least we can arrange three types of corrections where the first type comprises the corrections Eq. (*13*), Eq. (*14*), and Eq. (*15*), the second Eq. (*16*) and Eq. (*17*), and the third type contains the corrections Eq. (*18*) and Eq. (*19*). Since we are interested in the DGB method and these corrections are originally added to the CISD approach, as mentioned, therefore we have to employ the BD_2 scheme instead of CISD. Thus, we will designate these corrections as BD_2app, where app represents the abbreviations for the size-extensivity corrections used in Eqs (*13*)–(*19*). Moreover, we will apply these corrections to the approach we are focused on, the B0 scheme. For more insight into these corrections, we refer to the original literature and, e.g., ref.[17].

B. Spectroscopic Constants

To test the quality of the approximation schemes, especially in the neighborhood of the equilibrium geometry of the system considered, the spectroscopic constants, excitation energies, and ro-vibrational energy levels are good quantities for an assessment which can, moreover, be compared with available experimental data.

Now, a computed potential-energy curve (PEC) is best assessed by generating the ro-vibrational energies[26,27]. In order to do so, here we employ the LEVEL package of LeRoy[28], which solves the radial one-dimensional Schrödinger equation

$$-\frac{\hbar}{2\mu}\frac{\mathrm{d}^2\Psi_{v,J}(R)}{\mathrm{d}R^2} + V_J(R)\Psi_{v,J}(R) = E(v,J)\Psi_{v,J}(R) \qquad (20)$$

where $V_J(R)$ is given by a sum of the electronic potential energy (here represented by our computed PEC) and of a centrifugal term, to obtain the vibrational (v)–rotational (J) energy levels $E(v,J)$ for the molecular state considered, as well as the rotational constants B_v, D_v, and H_v which depend on the vibrational quantum number v (see below).

Then, the computed ro-vibrational energies $E(v,J)$, and the rotational constants, B_v, D_v, and H_v, can be used to determine other spectroscopic constants (with respect to the equilibrium geometry of the diatomic molecule) by relying on the Dunham expansion and the techniques used in the analysis of the experimental data. For this purpose we employ the following approximations for the ro-vibrational term values

$$\begin{aligned} E(v,J) &= G(v) + F_v(J) \\ G(v) &\approx \omega_e(v+1/2) - \omega_e x_e(v+1/2)^2 + \\ &\qquad \omega_e y_e(v+1/2)^3 + \omega_e z_e(v+1/2)^4 \\ F_v(J) &\approx B_v J(J+1) - D_v(J(J+1))^2 + H_v(J(J+1))^3 \end{aligned} \qquad (21)$$

and for the rotational constants

$$\begin{aligned} B_v &\approx B_e - \alpha_e(v+1/2) + \gamma_e(v+1/2)^2 \\ D_v &\approx \mathbf{D}_e + \beta_e(v+1/2) \\ H_v &\approx H_e \ . \end{aligned} \qquad (22)$$

We then compute the spectroscopic constants ω_e, $\omega_e x_e$, $\omega_e y_e$, $\omega_e z_e$, B_e, α_e, γ_e, $\mathbf{D}_e$, β_e, H_e using the difference method[11,26]. For instance, representing the vibrational values $G(v) = E(v,0)$ as polynomials in $x = v + 1/2$, namely $G(v) \equiv G(x - 1/2) \equiv G_x = \sum_{i=1}^{n} a_i x^i$, we obtain the k-th difference $\Delta^k G_x$ for any fixed value ξ of x by a linear combination of the spectroscopic constants a_i,

$$\Delta^k G_\xi := \Delta^{k-1} G_{\xi+1} - \Delta^{k-1} G_\xi = \sum_{i=1}^{n} c_i^{(k)}(\xi) a_i \tag{23}$$

with coefficients $c_i^{(k)}$ given by

$$c_i^{(k)}(\xi) = \sum_{j=0}^{k} (-1)^j \binom{k}{j} (k - j + \xi)^i \ . \tag{24}$$

This implies that for a chosen fixed value of n, the n-th coefficient a_n is given by the n-th difference $\Delta^n G_x$,

$$a_n = (n!)^{-1} \Delta^n G_x \quad \text{and} \quad \Delta^{(n+m)} G_x = 0 \,, \quad \text{for} \quad m = 1, 2, 3, \ldots . \tag{25}$$

Thus, assuming that the n-th difference of term values G_x are x- or v-independent, we then determine the desired a_i values, $i = 1, \ldots, n$ (or the spectroscopic constants $a_1 = \omega_e$, $a_2 = -\omega_e x_e$, ...) by solving the system of equations (*23*) choosing $\xi = 1/2$, i.e., $v = 0$. This is easily done via back-substitution. An analogous difference scheme is also applied to B_v, D_v, and H_v.

A further point of view to evaluate the quantity of the wave function of the underlying approximation is the determination of so-called response properties for a molecular system immersed in a weak field of interest. For instance, in the case of an electric field $\mathcal{E}$, these properties are the electric dipole moment μ or hyperpolarizabilities like α, β, or γ. The most straightforward method of computing these properties is the so-called finite-field (FF) method[29]. The energy change ΔE when the system is exposed to a homogeneous electric field along one direction can be written as

$$\begin{aligned} \Delta E &\equiv E(\mathcal{E}) - E(0) \\ &= -\mu \mathcal{E}^1 - \frac{1}{2!} \alpha \mathcal{E}^2 - \frac{1}{3!} \beta \mathcal{E}^3 - \frac{1}{4!} \gamma \mathcal{E}^4 \ \ldots \end{aligned} \tag{26}$$

where $E(0)$ designates the energy of the system with no field applied. For linear diatomic hydrides in a uniform electric field along the molecular axis – considering a weak field $\mathcal{E}$ – we can approximately evaluate the dipole moment μ, dipole polarizability α, or the hyperpolarizabilities up to the quartic term, β and γ, if we compute ΔE, Eq. (*26*), for a few values of an electric reference-field $\mathcal{E}$: 0, $\pm\mathcal{E}$, $\pm 2\mathcal{E}$, as follows[30]

$$\mu\mathcal{E}^1 = -\frac{2}{3}(E(+\mathcal{E}) - E(-\mathcal{E})) + \frac{1}{12}(E(+2\mathcal{E}) - E(-2\mathcal{E})) \qquad (27)$$

$$\alpha\mathcal{E}^2 = \frac{5}{2}E(0) - \frac{4}{3}(E(+\mathcal{E}) + E(-\mathcal{E})) + \frac{1}{12}(E(+2\mathcal{E}) + E(-2\mathcal{E})) \qquad (28)$$

$$\beta\mathcal{E}^3 = (E(+\mathcal{E}) - E(-\mathcal{E})) - \frac{1}{2}(E(+2\mathcal{E}) - E(-2\mathcal{E})) \qquad (29)$$

$$\gamma\mathcal{E}^4 = -6\,E(0) + 4(E(+\mathcal{E}) + E(-\mathcal{E})) - (E(+2\mathcal{E}) + E(-2\mathcal{E}))\,. \qquad (30)$$

The principal weakness of the FF approach stems from the contrary demands which are imposed on the numerical differentiation of the energy. On one hand, we have to use very small fields to obtain an accurate approach of the derivatives and, on the other hand, this requires a very high precision of the computed energies $E(\mathcal{E})$. Since analytical derivatives for the DGB methods (cf. h) of ref.[11]) are not yet implemented, therefore we are using the FF approach to calculate the dipole moment μ and the dipole polarizability α. If not explicitely mentioned in the following applications, we have chosen the reference field strength to be $\mathcal{E} = 0.002$ a.u. and the energy to be converged to at least 10^{-8} a.u.

III. APPLICATIONS

First, we will apply the DGB method addressed in Section I and Section II to the Li and Be atoms as well as to the molecules LiH and BeH. As recently shown, an encouraging DGB approach is BQ_2 which shows promise in different applications[11] such as, for instance, when dissociating the N_2 molecule where the CCSD method fails[10]. Here, in contrast to BQ_2, CCSD yields a potential energy curve with a huge hump at the intermediately stretched

geometries, especially in the single reference case when the restricted Hartree–Fock (RHF) configuration is used. However, since we are interested in simple methods to calculate physical and chemical properties of molecular systems, we will turn our attention to the DGB approach B0 and to derivatives of the B0 scheme as well. But in order to obtain an assessment of this approximation even for small molecules, where highly accurate calculations can be performed, we will consult besides BQ_2 also the sophisticated methods BD_2 and BQe_2 and, if applicable, the BQm_f approach. On the other hand, we even have to take into account simple calculation schemes which can be used to estimate correlation energies in the case of large molecules as the perturbation approach MP2. Moreover, to obtain an insight into the B0 method, we also compare the results with experimental values if available. Finally, we consider as mentioned the phenolate anion. Here, we only apply the B0 approach to the equilibrium geometry of the isolated anion to calculate the energies of the ground and low-lying excited states.

A. Application to Li and Be Atoms

We start our assessment of the B0 approach by considering a simple atomic system, the lithium atom. First we consider the ground state and the first seven excited states as well. Since we deal with a three-electron system and use a double-zeta basis set cc-pVDZ [32], it is practicable to perform a full configuration interaction (FCI), i.e. CISDT calculation. The results of the FCI and the deviations of the DGB approaches, mentioned above, as well as of the MP2 and size-extensivity BD_2 corrections of Eqs (*13*)–(*19*) are reported in Table I. Here, we used the relative and therefore dominant Slater determinant for the reference function of each state shown in Table I. Now, if we take a look on the differences of B0, Δ(B0), we see that for the first six states the B0 approach leads to nearly the same accuracy of energy. For the last two excited states $^2S(1s^1 2s^2)$ and $^4P(1s^1 2s^1 2p^1)$, the accuracy of the energy significantly deteriorates. This indicates the different characters of these states compared to the other states. In these cases the description of the reference state by one determinant is not anymore sufficient. If the reference state is at least built up by a linear combination of two determinants, the deviations can be reduced. Then, we obtain for the $^2S(1s^1 2s^2)$ state Δ(B0) = 9.142 mhartree and for $^4P(1s^1 2s^1 2p^1)$, Δ(B0) = 7.880 mhartree. Considering the C_0 coefficients of the reference states in the case of BD_2, given in Table I, and used in the size-extensivity corrections, the coefficients reflect the reference character of the states. Here, the values of the coefficients of the latter states are far less than 1.0 whereas the coefficients

TABLE I

Full CI energies[a] (FCI, in hartree) and deviations (Δ(app), in mhartree) from FCI energies of ground and excited states of the Li atom obtained with MP2 and various DGB approximations (app) using the cc-pVDZ[b] basis set

State	Δ(MP2)	Δ(B0)	$\Delta(BD_2)$[c]	$\Delta(BQ_2)$	$\Delta(BQe_2)$[d]	$\Delta(BQm_f)$	FCI[a]
$^2S(1s^22s^1)$	0.024	0.042	0.002	0.002	0.002	0.000	–7.433465
$^2P(1s^22p^1)$	1.249	0.199	0.059	0.011	0.007	0.000	–7.365816
$^2P(1s^23p^1)$	–1.156	0.092	0.038	–0.001	–0.004	0.000	–7.258238
$^2S(1s^23s^1)$	0.047	0.047	0.002	0.001	0.001	0.000	–7.248237
$^2D(1s^23d^1)$	0.004	0.058	0.001	0.001	0.001	0.000	–7.103624
$^2S(1s^24s^1)$	0.044	0.069	0.001	0.001	0.001	0.000	–6.758782
$^2S(1s^12s^2)$	–4.644	15.778	2.127	1.929	0.050	0.002	–5.340344
$^4P(1s^12s^12p^1)$	0.849	21.885	0.428	0.414	0.000	0.000	–5.288177

State	Δ(dc)[e]	Δ(rdc)[e]	Δ(dsc)[e]	Δ(pc)[e]	Δ(ddc)[e]	Δ(mc)[e,f]	C_0
$^2S(1s^22s^1)$	0.001	0.001	0.001	0.002	0.002	0.002	0.999
$^2P(1s^22p^1)$	–0.209	–0.221	0.235	–0.033	–0.036	0.059	0.955
$^2P(1s^23p^1)$	0.206	0.214	0.223	0.096	0.098	0.038	0.953
$^2S(1s^23s^1)$	0.000	0.000	0.000	0.001	0.001	0.002	0.999
$^2D(1s^23d^1)$	0.001	0.001	0.001	0.001	0.001	0.001	0.999
$^2S(1s^24s^1)$	0.001	0.001	0.001	0.001	0.001	0.001	0.999
$^2S(1s^12s^2)$	–23.244	–31.251	–46.644	–7.764	–10.307	2.127	0.760
$^4P(1s^12s^12p^1)$	–63.657	–120.110	–1011.652	–27.958	–56.454	0.428	0.532

[a] Obtained with GAMESS, see ref.[31]. [b] From ref.[32]. [c] For ground states BD_2 is equivalent to CISD. [d] For ground states BQe_2 is equivalent to CCSD. [e] Correlation-energy corrections based on BD_2 (i.e. BD_2app, see text). [f] For three-electron systems mc corrections (i.e. BD_2mc, as well as BD_2msc) are equivalent to BD_2.

of the remaining states are close to the value of 1.0. A closer look reveals that the first two excited states show a small deviation of the one determinant character which is also reflected in the results of the DGB approaches and the size-extensivity corrections as well. Here, one can observe that the corrections of BD_2 do not improve the energy, even more deteriorate the energy of the excited states which show a multi-determinant character of the reference function. The results of the size-corrections of BD_2 also show, as already mentioned, the three kinds of corrections: 1. BD_2dc, BD_2rdc, BD_2dsc; 2. BD_2pc, BD_2ddc; and 3. BD_2mc, BD_2msc. It should also be mentioned that in this case of a three-electron system, the results of BD_2mc are equivalent to BD_2, which also holds for BD_2msc.

In comparison to the B0 approach, the MP2 approach does not give consistent results. To complete the consideration, Table I also shows the results of the BD_2, BQ_2, and BQe_2, as well as the BQm_f approach. As might be expected, we observe that BQm_f leads to results of almost FCI accuracy. Thus, we have the following hierarchy B0 < BD_2 < BQ_2 < BQe_2 < BQm_f whereas MP2 overall shows a quite different and less satisfying quality of the results.

Next, we consider the α and γ polarizabilities of the Li atom. The computed total energies and the dipole polarizabilities, α, as well as the hyperpolarizability, γ, obtained with various methods are compared with experimental values in Table II. Since the computation of the hyperpolarizability, particularly when using the FF method, is more challenging with respect to the basis set and the accuracy of the energy, we are thus employing the fairly large quadruple zeta basis set cc-pVQZ [32] and, as mentioned, we required that the energy is accurate to at least 10^{-8}. Furthermore, in order to obtain an insight into the stability of the calculation performed, we exploit two different strengths of the reference field $\mathcal{E}$, namely $\mathcal{E} = 0.001$ a.u. and $\mathcal{E} = 0.002$ a.u. Considering the results of α of Table II, one can state that except B0[D_2,D_2] all approaches are showing relatively stable results with respect to the reference filed $\mathcal{E}$. This also holds for the γ values if we ignore the internal corrected B0 approximations. Here, we obtain an unstable behavior which is also shown by the FCI values, however, not at the same scale. These results seem to indicate that we can rely more on the larger reference field $\mathcal{E} = 0.002$ than on smaller reference fields if at all when considering higher-order properties (cf. ref.[33]). Thus, as already mentioned and for the sake of comparison, we shall use in the following calculation of dipole moments (μ_e at the equilibrium geometry) the reference field $\mathcal{E} = 0.002$.

Now, the computed total energies show expected results: the SCF energy covers 99.5621% of the FCI energy and 99.3934% of the estimate of the exact energy[35], a deviation in the order of magnitude of about 0.5%. Com-

paring the values of the MP2 approach and the B0 approach, either of them recovers almost the entire correlation energy: MP2 99.9427% of FCI (99.7734% of the exact energy) and B0 99.9704% of FCI (99.801% of the exact energy). However, the B0 approximation can be improved by the internal corrections, especially if we consider the B0[D_2,D_2] (99.9994% of FCI) which in this case is almost the result of the CISD equivalent BD_2. Con-

TABLE II

Energies (E, in hartree) and polarizabilities α and γ (in a.u.) of the Li atom obtained with various methods and the quadruple zeta basis sets cc-pVQZ[a] based on the finite field method[b] (the strength x of the reference field $\mathcal{E}$ are given in a.u., $\mathcal{E}(x)$; numbers in parentheses of the γ values give the exponents in base 10)

Method	E	$\mathcal{E}(0.001)$		$\mathcal{E}(0.002)$	
		α	γ	α	γ
SCF	–7.432697	170.00	–6.8620(+05)	169.99	–6.2989(+05)
MP2	–7.461114	165.10	–5.7554(+05)	165.09	–5.2710(+05)
B0	–7.463181	164.37	–5.6045(+05)	164.36	–5.0975(+05)
B0[–,D_2]	–7.465178	164.47	1.0510(+06)	165.00	–5.3193(+05)
B0[D_2,–]	–7.465192	164.41	1.2440(+06)	165.00	–5.2951(+05)
B0[D_2,D_2]	–7.465345	159.61	9.8899(+06)	165.27	–6.6380(+05)
BD_2	–7.465358	165.03	–5.0979(+05)	165.04	–5.2855(+05)
BQ_2	–7.465359	165.06	–5.1258(+05)	165.07	–5.3063(+05)
BQe_2	–7.465359	165.06	–5.1286(+05)	165.07	–5.3075(+05)
BQm_f	–7.465386	164.97	–5.0943(+05)	164.97	–5.2802(+05)
BD_2dc	–7.465475	164.99	–5.0904(+05)	165.00	–5.2883(+05)
BD_2rdc	–7.465475	164.99	–5.0904(+05)	165.00	–5.2884(+05)
BD_2dsc	–7.465476	164.99	–5.0904(+05)	165.00	–5.2884(+05)
BD_2pc	–7.465397	165.02	–5.0954(+05)	165.03	–5.2864(+05)
BD_2ddc	–7.465397	165.02	–5.0954(+05)	165.03	–5.2864(+05)
BD_2mc[c]	–7.465358	165.03	–5.0979(+05)	165.04	–5.2855(+05)
FCI[d]	–7.465389	164.95	–4.7200(+05)	164.97	–5.3188(+05)
Estimate[e]	–7.478062[f]	164.00		164.00	

[a] From ref.[32] [b] See ref.[30] [c] For three-electron systems BD_2mc and BD_2msc are equivalent to BD_2. [d] Obtained with GAMESS[31]. [e] From ref.[34] [f] The most recent nonrelativistic estimate of the exact energy[35].

sidering the corrected BD_2 results, from BD_2dc to BD_2mc, we can here identify the same groups of corrections as before. Here, it should be stressed that all corrected BD_2 results, except BD_2mc, overestimate the energy of the FCI calculation. The best estimation of the ground state energy is given by the BQm_f approach. This also holds for the polarizabilities α and γ.

Besides the Li atom, we now assess the B0 approach at a next simple atomic system which represents a closed-shell system, the Be atom. The results of the ground state and few excited states are shown in Table III. Here, besides the B0 approach, as in the case of the Li atom, we also report the results of different levels of the DGB scheme and the MP2, the size-corrected BD_2 approaches and the FCI values as well. Moreover, we used the [7s3p1d] basis set[36]. In the case of the FCI results we only obtained an estimate of the energy of the $^3P(2s^13p^1)$ excited state since the FCI calculation did not converge for this state. It means that we have to be cautious about the deviations with regard to this state. Here, the BQm_f should represent a reasonable result if we take into account the results and the deviations of the energies of the other states. Considering the deviations of the B0 approach, we obtain a systematic – here underestimating – representation of the excited states which is correlated to the coefficient C_0 of the reference state of the BD_2 mirrored also in the results of the size-corrected approaches. The larger the deviation of the coefficient C_0 with respect to 1.0, the larger the error. This also indicates as in the case of Li atom that the reference state has to be represented by a larger reference space than used. In this context the $^1S(2p^2)$ stands for a state which at least needs a three-dimensional reference space to reach a reasonable result. Comparing the results of the MP2 and B0 approaches, Table III shows clearly without ambiguity the better performance of the B0 approach. Moreover, considering the other DGB approximations aside from BQm_f, the BQ_2 represents overall a reasonable approach for ground and excited states as well although the BQe_2 leads to a better result for the ground state. Also here we can recognize the structure of the C_0 coefficients. Finally, if we take a look at the BD_2 approach and its corrections, the second part of Table III gives the impression that the corrections of BD_2 do not always lead to improved results, far more they lead to deteriorated values for the excited states. The only exceptions are given by the BD_2mc and BD_2msc estimates.

B. Application to the LiH Molecule

Although we are in the long run interested in larger molecules, we here apply our simple approach B0 to simple systems to get an idea of the perfor-

TABLE III
Full CI energies[a] (FCI, in hartree) and deviations (Δ(app), in mhartree) from FCI energies of ground and excited states of the Be atom obtained with MP2 and different DGB approximations (app) using the [7s3p1d][b] basis set

State	Δ(MP2)	Δ(B0)	Δ(BD_2)[c]	Δ(BQ_2)	Δ(BQe_2)[d]	Δ(BQm_f)	FCI[a]
$^1S(2s^2)$	19.980	2.118	1.545	0.327	0.241	0.025	–14.634890
$^3P(2s^12p^1)$	8.884	8.883	2.034	0.328	0.756	0.112	–14.533527
$^1P(2s^12p^1)$	10.830	2.428	1.124	0.063	0.313	–0.059	–14.431321
$^3S(2s^13s^1)$	8.717	4.589	1.130	0.239	0.464	0.086	–14.377601
$^3P(2p^2)$	–1.873	9.269	3.425	0.457	5.585	0.507	–14.359603
$^1S(2s^13s^1)$	12.197	3.381	1.554	0.167	0.507	–0.014	–14.354369
$^1D(2p^2)$	–38.599	11.367	4.028	0.371	6.678	0.467	–14.352995
$^1P(2s^13p^1)$	24.163	15.304	6.263	1.182	2.410	0.144	–14.276303
$^1S(2p^2)$[e]	–	–	–	–	–	–	–14.273123
$^3P(2s^13p^1)$	–3.823	–4.834	–13.579	–16.150	–10.903	–16.377	(–14.248049)[f]

State	Δ(dc)[g]	Δ(rdc)[g]	Δ(dsc)[g]	Δ(pc)[g]	Δ(ddc)[g]	Δ(mc)[g]	Δ(msc)[g]	C_0
$^1S(2s^2)$	–3.722	–4.226	–4.835	–1.333	–1.485	0.584	0.754	0.91
$^3P(2s^12p^1)$	–3.898	–4.653	–5.626	–1.296	–1.536	0.920	1.151	0.89
$^1P(2s^12p^1)$	–2.421	–2.676	–2.972	–0.774	–0.847	0.491	0.636	0.93
$^3S(2s^13s^1)$	–1.239	–1.396	–1.576	–0.132	–0.176	0.709	0.779	0.94
$^3P(2p^2)$	–11.977	–15.528	–21.208	–5.929	–7.287	0.266	1.086	0.81
$^1S(2s^13s^1)$	–3.083	–3.564	–4.156	–0.998	–1.145	0.701	0.869	0.91
$^1D(2p^2)$	–20.028	–27.478	–41.612	–11.364	–14.611	–1.233	0.213	0.76
$^1P(2s^13p^1)$	–21.313	–35.938	–83.596	–13.532	–22.453	–0.771	2.469	0.65
$^1S(2p^2)$[e]	–	–	–	–	–	–	–	(0.56)
$^3P(2s^13p^1)$	–14.046	–14.144	–14.296	–13.858	–13.895	–13.673	–13.618	0.82

[a] Obtained with GAMESS [31]. [b] From ref.[36] [c] For ground states BD_2 is equivalent to CISD. [d] For ground states BQe_2 is equivalent to CCSD. [e] Here, at least, a three-dimensional reference space is needed (see text). [f] No convergence reached (see text). [g] Correlation-energy corrections based on BD_2 (i.e. BD_2app, see text).

mance of this approximation scheme where highly accurate results are available – be it from the experimental or computational side. First of all, in order to follow the first parts, we consider the LiH molecule. To assess the B0 approach we have calculated the potential energy curves (PECs) obtained with the correlated basis sets cc-pV(D,T,Q)Z [32]. Based on these PECs spectroscopic constants, as described in Eqs (*21*) and (*22*), the dipole moments at the equilibrium geometries and the dissociation energies as well are reported at the B0 level in Table IV. For comparison different DGB approximations, as described in Section II.A, MP2 and FCI values as well as experimental results are shown in Table IV. Here, it should be stressed that the dissociation energies reported in the Tables are calculated from the difference of the energies at the equilibrium geometries of the molecule and the sum of the energies of the atoms in the ground states (infinite separation), i.e. $D_e = E(\mathrm{Li}) + E(\mathrm{H}) - E(\mathrm{LiH}_{eq})$ (in cm^{-1}). The dipole moments are obtained with the FF method as described in the last section. In addition to the standard DGB approximations the size-extensivity corrections of the BD_2 approach (BD_2app) and the internal-corrected B0 approach, based on the C_0 coefficients, obtained with a two-determinant reference state are reported in Table V (e.g. 2D-B0[D_2,D_2]msc or for short B0-2msc, where msc stands for the abbreviation of the corrections introduced in Section II, i.e. for the Molnar–Szalay correction, Eq. (*19*)). Moreover, the FCI energies and the deviations with respect to the FCI values of selected DGB approaches for various internuclear separations are listed in Table VI, here obtained with the correlated basis sets cc-pVDZ and cc-pVTZ [32].

First of all, we regard the advanced DGB approaches of Table IV. Here, we have the situation that, with respect to the basis sets, the results of BD_2 to BQ_4 are almost equivalent. Especially, looking at the results of the BQ_4 approach, we cover almost the values of the FCI calculation, which also holds for the experimental results. Thus, the missing FCI results of the cc-pVQZ basis set should be close to the results of the BQ_4 approach.

Next, considering the B0 approach – also with regard to the MP2 results – we obtain a satisfying agreement with the experimental values. However, the results of ω_e and $\omega_e x_e$ unfortunately deteriorate with increasing number of basis functions in contrast to the MP2 results. Here, the MP2 yields a slightly better behavior in the range of the equilibrium geometry but with the addition that the MP2 method leads to an unstable PEC in the dissociation range of the geometry, as shown in Fig. 1 for the results obtained with the cc-pVTZ basis set. Besides the B0 and MP2 PECs, Fig. 1 pictures also two further approaches of Table IV, i.e. B0[D_2,D_2] and 2D-B0[D_2,D_2] which are based on the B0 method. Obviously, these internal-corrected approaches do

TABLE IV

Experimental results and computed spectroscopic constants (in cm^{-1}, μ_e in D, R_e in Å) for the LiH molecule, obtained with different approximations using different correlated basis sets (the numbers in parentheses give the exponents in base 10)

Method	Basis set[a]	$-\mu_e$	D_e	R_e	ω_e	$\omega_e x_e$	B_e	α_e	$\mathbf{D}_e$
B0	cc-pVDZ	5.80	17939.7	1.6123	1403.41	16.11	7.3591	0.1668	0.8094(–3)
	cc-pVTZ	5.73	14970.0	1.5932	1459.44	38.12	7.5366	0.2117	0.8198(–3)
	cc-pVQZ	5.84	19153.6	1.5978	1489.56	52.93	7.4927	0.1787	0.7880(–3)
MP2[b]	cc-pVDZ	5.85	16457.4	1.6089	1403.04	19.52	7.3897	0.1794	0.8204(–3)
	cc-pVTZ	5.88	18103.5	1.5893	1446.50	24.83	7.5733	0.2094	0.8323(–3)
	cc-pVQZ	5.89	18455.5	1.5919	1439.63	22.47	7.5486	0.1961	0.8313(–3)
B0[D_2,–]	cc-pVDZ	5.78	18139.6	1.6073	1395.95	21.34	7.4049	0.1855	0.8355(–3)
	cc-pVTZ	5.87	19537.9	1.5909	1436.83	26.86	7.5582	0.2157	0.8403(–3)
	cc-pVQZ	5.87	19580.1	1.5948	1439.51	29.11	7.5215	0.1946	0.8293(–3)
B0[–,D_2]	cc-pVDZ	5.79	18135.2	1.6072	1396.21	21.22	7.4057	0.1852	0.8353(–3)
	cc-pVTZ	5.87	19551.3	1.5908	1437.16	26.88	7.5589	0.2156	0.8402(–3)
	cc-pVQZ	5.87	19571.9	1.5947	1440.14	29.23	7.5225	0.1946	0.8291(–3)
B0[D_2,D_2]	cc-pVDZ	5.73	18276.2	1.6099	1382.13	20.97	7.3805	0.1896	0.8423(–3)
	cc-pVTZ	5.86	19796.2	1.5927	1425.22	25.54	7.5408	0.2203	0.8457(–3)
	cc-pVQZ	5.86	19884.0	1.5960	1423.88	26.83	7.5100	0.2029	0.8410(–3)
2D-B0[D_2,D_2]	cc-pVDZ	5.75	18280.5	1.6102	1381.13	21.03	7.3782	0.1900	0.8427(–3)
	cc-pVTZ	5.84	19794.9	1.5928	1424.78	26.30	7.5397	0.2206	0.8469(–3)
	cc-pVQZ	5.86	19883.7	1.5961	1421.52	25.05	7.5094	0.2042	0.8411(–3)
BD_2	cc-pVDZ	5.74	18298.4	1.6107	1377.63	21.77	7.3735	0.1934	0.8454(–3)
	cc-pVTZ	5.82	19834.6	1.5932	1421.94	26.55	7.5363	0.2228	0.8489(–3)
	cc-pVQZ	5.85	19932.2	1.5964	1415.85	24.02	7.5063	0.2072	0.8453(–3)
BQ_2	cc-pVDZ	5.74	18304.8	1.6107	1377.32	21.78	7.3740	0.1932	0.8460(–3)
	cc-pVTZ	5.82	19935.3	1.5937	1419.41	26.91	7.5317	0.2246	0.8505(–3)
	cc-pVQZ	5.84	20122.8	1.5978	1410.53	24.62	7.4927	0.2094	0.8473(–3)
BQe_2	cc-pVDZ	5.75	18305.2	1.6106	1377.31	21.79	7.3740	0.1932	0.8460(–3)
	cc-pVTZ	5.82	19944.1	1.5937	1419.19	26.88	7.5314	0.2247	0.8506(–3)
	cc-pVQZ	5.83	20142.3	1.5979	1409.59	24.51	7.4919	0.2100	0.8479(–3)
BQ_4	cc-pVDZ	5.73	18308.0	1.6106	1377.24	21.78	7.3742	0.1932	0.8461(–3)
	cc-pVTZ	5.81	19951.0	1.5936	1419.39	26.96	7.5330	0.2248	0.8510(–3)
	cc-pVQZ	5.83	20142.3	1.5976	1410.39	24.65	7.4945	0.2095	0.8481(–3)
FCI	cc-pVDZ	5.73	18317.9	1.6106	1377.21	21.79	7.3742	0.1932	0.8462(–3)
	cc-pVTZ	5.81	20208.7	1.5936	1419.11	26.93	7.5327	0.2248	0.8512(–3)
	cc-pVQZ	–	–	–	–	–	–	–	–
Exp.[c]		5.88	19589.4	1.5957	1405.65	23.20	7.5131	0.2132	0.8617(–3)

[a] From ref.[32] [b] Obtained from an 'unstable' local minimum of the PEC (see text). [c] From refs[26,37], μ_e from ref.[38], D_e from ref.[39]

TABLE V

Experimental results and computed spectroscopic constants (in cm^{-1}, μ_e in D, R_e in Å) for the LiH molecule, obtained with different approximations using the correlated basis set (the numbers in parentheses give the exponents in base 10)

Basis set[a]	Method[b,d]	$-\mu_e$	D_e	R_e	ω_e	$\omega_e x_e$	B_e	α_e	$\mathbf{D}_e$
cc-pVTZ	BD_2dc	5.79	20174.7	1.5952	1411.30	27.62	7.5174	0.2291	0.8554(–3)
	BD_2rdc	5.79	20185.5	1.5954	1410.59	27.71	7.5160	0.2295	0.8558(–3)
	BD_2dsc	5.79	20196.9	1.5955	1409.81	27.82	7.5146	0.2300	0.8563(–3)
	BD_2pc	5.81	20011.2	1.5943	1416.29	27.12	7.5262	0.2261	0.8523(–3)
	BD_2ddc	5.81	20014.0	1.5943	1416.10	27.14	7.5259	0.2262	0.8525(–3)
	BD_2mc	5.82	19894.3	1.5936	1420.06	26.74	7.5329	0.2239	0.8501(–3)
	BD_2msc	5.82	19890.1	1.5935	1420.25	26.72	7.5333	0.2238	0.8500(–3)
	B0-2dc	5.82	19788.0	1.5945	1415.81	27.09	7.5237	0.2256	0.8523(–3)
	B0-2rdc	5.81	19788.0	1.5947	1415.23	27.15	7.5226	0.2259	0.8527(–3)
	B0-2dsc	5.81	19787.9	1.5948	1414.59	27.22	7.5213	0.2263	0.8530(–3)
	B0-2pc	5.83	19792.9	1.5937	1420.02	26.71	7.5312	0.2232	0.8498(–3)
	B0-2ddc	5.83	19792.9	1.5938	1419.86	26.73	7.5309	0.2233	0.8498(–3)
	B0-2mc	5.84	19795.3	1.5931	1423.19	26.43	7.5369	0.2215	0.8478(–3)
	B0-2msc	5.84	19795.3	1.5931	1423.35	26.42	7.5372	0.2214	0.8478(–3)
cc-pVQZ	BD_2dc	5.81	20367.2	1.5993	1402.46	25.04	7.4794	0.2135	0.8523(–3)
	BD_2rdc	5.81	20381.6	1.5995	1401.55	25.14	7.4776	0.2140	0.8528(–3)
	BD_2dsc	5.81	20396.9	1.5997	1400.55	25.24	7.4755	0.2146	0.8533(–3)
	BD_2pc	5.83	20161.1	1.5979	1408.75	24.56	7.4921	0.2105	0.8490(–3)
	BD_2ddc	5.83	20164.9	1.5980	1408.50	24.59	7.4916	0.2107	0.8491(–3)
	BD_2mc	5.84	20011.4	1.5969	1413.49	24.20	7.5016	0.2083	0.8465(–3)
	BD_2msc	5.84	20007.5	1.5968	1413.68	24.18	7.5020	0.2082	0.8464(–3)
	B0-2dc	5.83	19858.2	1.5986	1410.76	26.16	7.4859	0.2092	0.8447(–3)
	B0-2rdc	5.83	19858.0	1.5987	1410.05	26.25	7.4844	0.2096	0.8468(–3)
	B0-2dsc	5.83	19857.9	1.5989	1409.27	26.35	7.4826	0.2100	0.8472(–3)
	B0-2pc	5.84	19875.3	1.5974	1415.81	25.64	7.4970	0.2068	0.8439(–3)
	B0-2ddc	5.84	19875.3	1.5974	1415.62	25.66	7.4965	0.2070	0.8440(–3)
	B0-2mc	5.85	19883.9	1.5965	1419.62	25.25	7.5053	0.2051	0.8420(–3)
	B0-2msc	5.86	19883.9	1.5965	1419.77	25.23	7.5056	0.2050	0.8420(–3)
	Exp.[c]	5.88	19589.4	1.5957	1405.65	23.20	7.5131	0.2132	0.8617(–3)

[a] From ref.[32] [b] Obtained from an 'unstable' local minimum of the PEC (see text). [c] From refs[26,37], μ_e from ref.[38], D_e from ref.[39] [d] Here, e.g. BD_2msc (B0-2msc) stands for msc-type of correlation-energy corrections based on BD_2 (2D-B0[D_2,D_2], see text).

improve the results of the B0 approximation substantially in the entire range of our calculation. Here, 2D-B0[D_2,D_2] represents the extension of B0[D_2,D_2] which is based on a reference state built up of two determinants.

Taking into account the size-extensivity corrections, mentioned above, we obtain results which are reported in Table V for the cc-pV(T,Q)Z basis sets. Especially for the cc-pVTZ basis set the PECs of these approaches are also pictured in Figs 2 and 3. First of all, Table V shows the results of the

TABLE VI
Energy deviations (in mhartree) from FCI[a] (in hartree) of the LiH molecule for various internuclear separations *R* (in a.u.), obtained with MP2 and DBG approximations using the correlated basis sets cc-pVDZ[b] and cc-pVTZ[b]

R	MP2	B0	B0-1[c]	B0-2[d]	MSC_o[e]	BD_2	BQ_2	BQe_2	BQ_4	FCI
cc-pVDZ										
2.00	9.753	3.084	0.233	0.252	0.101	0.158	0.053	0.044	0.011	–7.945661
2.90	8.451	1.783	0.135	0.125	–0.001	0.050	0.019	0.018	0.003	–8.015452
3.02	8.455	1.730	0.142	0.128	0.001	0.048	0.019	0.017	0.003	–8.016146
3.10	8.474	1.716	0.149	0.133	0.004	0.048	0.019	0.017	0.003	–8.016066
4.00	9.596	2.960	0.431	0.359	0.178	0.055	0.021	0.018	0.004	–7.999092
5.00	13.143	7.191	1.704	1.357	1.012	0.095	0.031	0.027	0.008	–7.971952
6.00	19.920	14.369	5.114	3.600	2.803	0.201	0.057	0.050	0.016	–7.951087
10.0	51.394	52.383	25.079	3.098	–2.043	0.594	0.153	0.161	0.040	–7.933030
13.0	35.372	53.331	27.676	2.127	–1.366	0.603	0.168	0.015	0.036	–7.932761
15.0	14.548	50.635	27.536	1.635	–1.268	0.599	0.171	0.003	0.035	–7.932747
cc-pVTZ										
2.00	11.101	5.094	0.818	0.869	0.620	0.660	0.210	0.167	0.057	–7.970043
2.90	10.766	4.423	0.742	0.782	0.540	0.600	0.147	0.108	0.051	–8.039580
3.02	10.824	4.395	0.754	0.791	0.546	0.605	0.145	0.105	0.051	–8.040028
3.10	10.875	4.406	0.764	0.800	0.552	0.609	0.144	0.104	0.052	–8.039783
4.00	12.132	5.569	1.129	1.117	0.800	0.759	0.159	0.107	0.066	–8.021611
5.00	14.987	8.517	2.343	2.175	1.687	1.239	0.243	0.146	0.119	–7.993568
6.00	20.096	13.892	5.608	4.774	3.936	2.441	0.440	0.249	0.242	–7.971030
10.0	51.073	50.566	30.940	10.517	4.812	9.686	1.414	0.435	0.841	–7.949413
13.0	43.533	57.302	35.124	7.924	2.766	10.157	1.501	0.043	0.840	–7.949098
15.0	28.035	56.879	35.234	6.878	2.371	10.075	1.513	0.029	0.822	–7.949084

[a] Obtained with GAMESS [31]. [b] From ref.[32] [c] Here, B0-1 stands for B0[D_2,D_2] (see text). [d] Here, B0-2 stands for 2D-B0[D_2,D_2] (see text). [e] Here, MSC_o stands for 2D-B0[D_2,D_2]msc (see text).

spectroscopic constants of the size-extensivity corrections based on the BD_2. Here, we also applied the size-extensivity corrections to the 2D-B0[D_2,D_2] approach which are represented as B0-2app in Table V. Obviously, there are no decisive differences in the results of the BD_2app corrections and the BD_2 values of Table IV if we focus on the range about the equilibrium geometry. Of course, LiH is a small system and the basis sets are large enough to cover the essential correlation contribution in this area to obtain results close to the experimental results. This also holds for the B0-2app corrections. However, if we take a look at the dissociation range from 6 to 15 a.u., as shown in Fig. 2 for the BD_2app approaches (given as APP) and Fig. 3 for the B0-2app approaches (given as APP_0), one can see the essentially different behavior of these approaches. If we consider the PECs

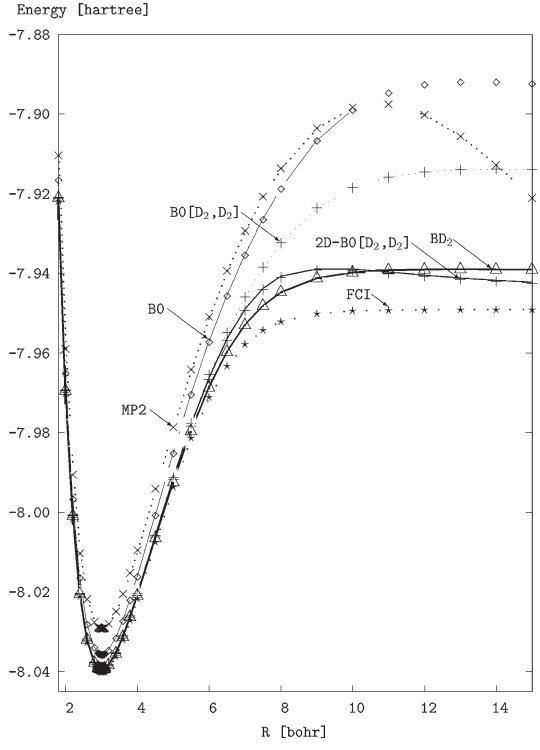

FIG. 1
Potential energy curves for the LiH ground state, obtained with the MP2, B0, B0[D_2,D_2], 2D-B0[D_2,D_2], BD_2, and FCI approximations and the cc-pVTZ basis set

of the size-extensivity corrections of BD_2 in Fig. 2, all corrections – except MSC – show instable performances in the dissociation range. This kind of performance deteriorates in the following oder (MSC <) MC < PC < DC < DDC < RDC < DSC. Here, the BD_2msc (MSC) outperforms all of the other approaches compared to the FCI-PEC. However, if we examine the results of the 2D-B0[D_2,D_2]-based corrections in Fig. 3, we obtain a similar behavior (MC_o < MSC_o < PC_o < DC_o < DDC_o < RDC_o < DSC_o) but even less worse than in the former case. Moreover, the Molnar–Szalay correction – be it applied to the BD_2 approach or even to the 2D-B0[D_2,D_2] approach – leads to satisfying results over the entire range of the internuclear separation. For completeness, Table VI shows the FCI energies and the energy deviations for B0 approaches we are interested in, as well as selected approaches for compari-

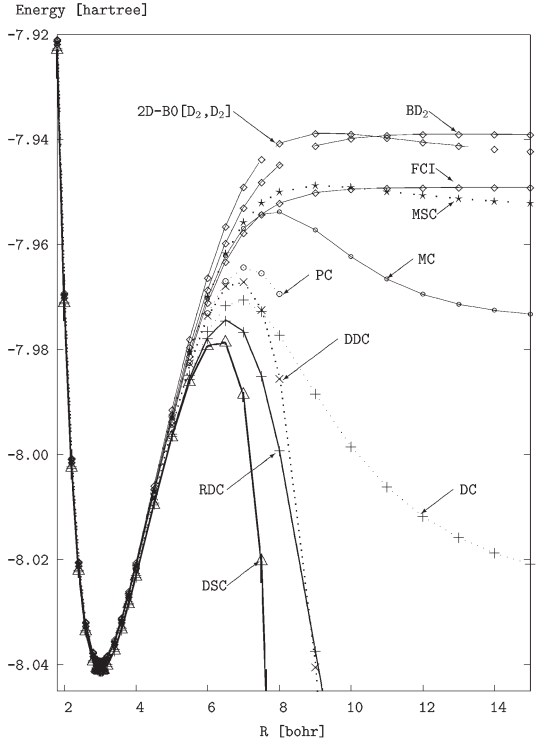

FIG. 2
Potential energy curves for the LiH ground state, obtained with the 2D-B0[D_2,D_2], BD_2, the BD_2-based size-extensivity approximations, as well as the FCI method and the cc-pVTZ basis set

son of various internuclear separations over the considered range obtained with the cc-pV(D,T)Z basis sets. Here, we can see – starting from B0 to MSC_o – the improvements of the absolute energy values displayed in the decreasing of the deviations. Especially, if we compare the results of the MP2 approach and the B0 approach. This also holds if we consider the results of MSC_o obtained with the cc-pVTZ basis set in comparison with the BD_2 approach.

Of course, besides the spectroscopic constants considered – in most cases representing the behavior of the internuclear separation range above the equilibrium geometry – we also have to take a look at the shape of the PEC at the intermediate range of internuclear separation. Here, one can consider the vibrational energy levels compared with the experimental results. These

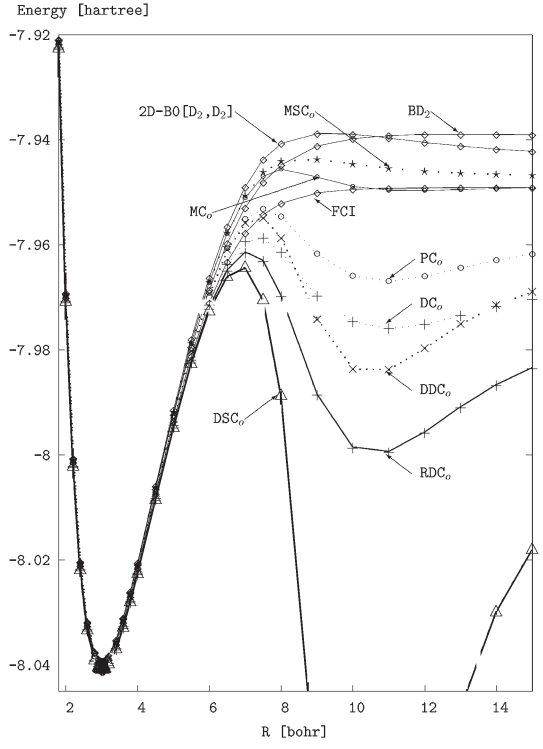

FIG. 3

Potential energy curves for the LiH ground state, obtained with the 2D-B0[D_2,D_2], BD_2, the 2D-B0[D_2,D_2]-based size-extensivity approximations, as well as the FCI method and the cc-pVTZ basis set

results based on the cc-pVTZ basis set for LiH are shown in Table VII. As in Table VI, we list the deviation with respect to the experimental results of the B0, B0[D_2,D_2] (cited as B0-1), 2D-B0[D_2,D_2] (cited as B0-2), and the corrected approach 2D-B0[D_2,D_2]msc (cited as MCS_o) compared with the MP2 approach and various higher-level DGB and CC approaches as well. At first sight we obtain for B0 and MP2 similar results where the MP2 values are based only on the local minimum of the PEC. Here, as before, improvements of B0 can be seen if we compare the approximation in the order B0, B0-1, B0-2, and MSC_o. When assessing the B0-based approaches: B0-1, B0-2, and MSC_o, the substantial improvement is obtained with the incorporation of the internal corrections based on the BD_2 approach. On the other hand, the influence of the second determinant in the reference state, B0-2, and even the size-extensivity correction, MSC_o, lead to small corrections whereas they are more important in the range of dissociation (cf. Fig. 1 and Fig. 3). For low-lying levels ν, the deviation errors with regard to BD_2 are about 70% for B0 and MP2, and have been reduced to about 30% in the case of B0-1 and about 15% for MSC_o. If we take also into account the middle part of the energy levels, the errors are increasing from about 70 to 76% for B0, from about 30 to 50% for B0-1, and from about 15 to 37% in the case of MSC_o. Then for higher-lying levels, the errors are still increasing for B0-1 up to 55% whereas the errors of the deviations are decreasing to about 70% in the case of B0 but about 30% for MSC_o. It should be stated that the absolute errors of B0 (BD_2) with regard to the experimental results are increasing from about 4% (1%) up to about 12% (3.5%) by increasing ν. This shows that the B0 approximations employed in Table VII – as mentioned – are not feasible approaches when chemical accuracy is required. However, with respect to computational demanding these approaches may be suitable to obtain semiquantitative results for large systems. Here, for instance, the relative computation time (without SCF calculation and four-index transformation) with respect to that required by the BD_2 approximation (T_r = 1.0) yields $T_r \approx 0.15$ for B0 and yields $T_r \approx 0.37$ for B0-1 by including the internal corrections, which is still inexpensive. That means one can save considerably computational time, i.e. about 80% in the case of B0 by increasing the error of only about 12%.

In order to complete these considerations, Table VIII shows the fundamental ($\nu \rightarrow \nu + 1$) vibrational transition energies of LiH, here obtained with the cc-pVQZ basis set to achieve an improvement with respect to the experimental data. As in the case of the vibrational energy levels of Table VII, we are reporting the deviation of MP2 and the suitable B0 approximation as well as of selected DGB, CC, and CI approaches for the assessment of the

TABLE VII

Experimentally based vibrational energy levels[a] (Exp.) of LiH and the differences between the FCI[b], 4R-RMR[b] (RMR), CCSD[b], MP2[c], as well DGB computed values and the experimental ones, obtained with the cc-pVTZ basis[d]. All values are in cm^{-1}

v	Exp.[a]	MP2[c]	B0	B0-1[e]	B0-2[e]	MSC_o[e]	BD_2	BQ_2	BQe_2	CCSD[b]	RMR[b]	FCI[b]
0	697.9	19.6	20.2	8.2	7.7	7.0	6.3	5.0	4.9	4.1	4.0	4.0
1	2057.6	58.7	57.4	24.4	22.6	20.2	17.6	13.1	12.8	11.9	11.8	11.7
2	3372.5	98.0	94.1	39.0	35.8	31.6	26.2	18.0	17.3	16.5	16.2	16.0
3	4643.4	139.7	137.4	54.0	49.6	43.2	34.2	21.7	20.6	19.8	19.3	18.9
4	5871.1	185.2	183.5	71.1	65.2	56.2	43.1	25.5	23.9	22.9	22.3	21.7
5	7056.6	235.4	232.1	90.8	83.1	71.6	53.4	30.0	27.7	26.8	25.9	25.0
6	8200.4	291.1	286.4	114.7	104.6	90.1	65.7	35.5	32.5	31.6	30.4	29.1
7	9303.0	353.1	348.1	143.5	130.4	112.4	80.4	42.2	38.3	37.4	35.9	34.1
8	10364.7	422.0	418.5	177.8	161.1	139.2	97.6	50.1	45.1	44.1	42.2	39.9
9	11385.9	498.4	498.3	218.2	196.8	170.6	117.4	58.7	52.5	51.5	49.1	46.2
10	12366.4	583.1	588.3	265.5	238.3	207.3	140.0	67.9	60.2	59.2	56.2	52.5
11	13306.0	677.2	688.5	320.8	286.1	249.6	165.6	77.3	67.8	66.8	63.0	58.4
12	14204.1	781.7	798.5	385.4	341.1	298.1	194.4	86.2	74.7	73.7	69.0	63.2
13	15059.6	898.5	919.2	460.7	404.0	353.5	227.0	94.3	80.3	79.2	73.3	66.2
14	15870.8	1029.7	1052.9	548.5	475.9	416.4	264.2	100.9	83.8	82.8	75.2	66.4
15	16635.2	1178.3	1203.3	651.2	558.3	487.9	307.1	105.5	84.5	83.4	73.5	62.8
16	17349.5	1347.9	1374.8	772.1	653.2	569.2	357.4	107.1	81.1	80.1	67.0	53.9
17	18008.7	1544.0	1573.2	916.8	763.5	661.8	417.8	105.1	72.7	71.8	54.1	38.1
18	18606.6	1773.1	1805.3	1091.9	892.4	766.9	491.5	98.3	58.0	57.0	32.6	13.2
19	19134.5	2044.1	2080.0	1306.0	1043.8	884.3	583.6	85.8	35.6	34.7	–0.1	–23.1
20	19581.1	2368.4	2409.5	1570.2	1221.4	1007.0	700.8	67.0	5.2	3.7	–47.5	–73.8
21	19932.1	2760.6	2808.5	1898.5	–	1091.5	851.6	41.6	–37.0	–36.0	–114.7	–141.9
22	20169.8	3238.2	3295.4	2309.0	–	–	1046.8	11.2	–	–81.7	–205.6	–230.1

[a] From ref.[40] [b] From ref.[41] [c] Obtained from an 'unstable' local minimum of the PEC (see text). [d] From ref.[32] [e] See Table VI.

accuracy of the cruder B0-based approximations. As before, the results of the B0-based approaches follow a similar performance, a substantial improvement is achieved with the incorporation of the internal correction, namely B0-1, and further (slight) improvements are obtained with a two-determinant reference state (B0-2) and the B0-based size-extensivity correction (MSC_o). The same holds also for the transition frequencies for selected lines in the P and R branches of various vibrational bands reported in Table IX. Here, the computational efficiency of the B0 and B0-1 approxima-

TABLE VIII

Experimentally determined fundamental ($v \rightarrow v + 1$) vibrational transition energies[a] (Exp.) of LiH and the deviations of the computed values from the experimental ones as obtained with various methods and the cc-pVQZ basis set[b]. All values are in cm^{-1}

v	Exp.[a]	MP2[c]	B0	B0-1[d]	B0-2[d]	MSC_o[d]	BD_2	BQ_2	BQe_2	CCSD[e]	CCSD[f]	CI[g]	CI[h]
0	1359.7	39.1	45.2	14.3	13.8	11.7	9.3	2.8	2.0	2.0	1.8	–6.8	–14.9
1	1314.9	39.4	33.5	14.5	13.8	11.4	9.1	1.5	0.8	0.8	0.5	–5.9	–14.6
2	1270.9	41.7	36.4	17.1	15.5	12.9	9.9	1.3	0.5	0.5	0.2	–4.4	–14.2
3	1227.8	45.4	39.1	19.6	18.2	15.4	11.6	1.8	0.8	0.8	0.5	–4.2	–12.8
4	1185.4	50.3	42.9	23.1	21.4	18.3	13.8	2.7	1.5	1.5	1.2	–5.3	–10.8
5	1143.8	55.7	53.4	27.5	25.0	21.6	16.2	3.6	2.2	2.2	1.9	–8.2	–8.8
6	1102.6	62.0	65.6	32.6	29.2	25.5	19.0	4.6	2.9	2.9	2.5	–11.2	–7.2
7	1061.8	68.9	75.9	37.5	33.8	29.6	22.1	5.6	3.5	3.5	3.0	–10.8	–6.3
8	1021.2	76.4	82.8	42.4	38.7	34.2	25.6	6.4	4.0	4.0	3.4	–11.6	–6.0
9	980.5	84.8	88.6	48.3	44.4	39.4	29.7	7.3	4.5	4.5	3.7	–10.6	–5.7
10	939.6	94.0	95.4	56.3	51.0	45.4	34.5	8.2	4.8	4.8	3.8	–10.2	–5.4
11	898.1	104.6	105.0	66.6	58.7	52.4	40.4	9.2	5.1	5.0	3.8	–9.8	–5.1
12	855.5	116.8	117.3	78.8	68.0	60.9	47.5	10.4	5.3	5.2	3.7	–10.0	–4.5
13	811.2	131.2	132.1	92.3	79.1	71.1	56.5	11.7	5.4	5.4	3.3	–11.2	–3.7
14	764.4	148.6	149.6	107.9	92.7	83.8	67.8	13.4	5.5	5.5	2.7	–12.6	–2.8
15	714.2	169.8	170.7	127.1	109.6	99.3	82.4	15.4	5.5	5.5	1.7	–14.2	–1.9
16	659.3	196.0	197.5	152.1	130.8	118.5	101.0	17.8	5.4	5.5	0.0	–16.2	–1.1
17	597.9	229.1	231.9	185.0	158.1	143.1	125.4	21.3	5.5	5.5	–2.4	–19.4	–0.4
18	527.9	271.0	276.6	227.5	193.3	175.0	157.3	26.1	5.8	5.8	–6.0	–24.8	0.1
19	446.6	324.4	334.5	281.9	237.9	214.7	199.0	32.4	6.8	6.9	–11.4	–31.4	0.3
20	351.0	392.1	408.3	350.4	291.7	258.4	253.2	40.8	9.1	9.3	–20.2	–39.0	–0.6
21	237.7	477.6	499.1	435.8	352.3	–	322.8	53.6	–	15.4	–36.1	–48.2	–2.0

[a] From ref.[40] [b] From ref.[32] [c] Obtained from an 'unstable' local minimum of the PEC (see text). [d] See Table VI. [e] From ref.[41] [f] CCSD-[4R] from ref.[41] [g] CI/STF From ref.[42] [h] From ref.[43]

TABLE IX

The deviations of the transition frequencies of various DGB approximations and 4R-RMR CCSD[a] (RMR), obtained with the cc-pVQZ basis sets[b], from the experimental values[c] (Exp.) for selected lines in the P and R branches of various vibrational bands of LiH. In each branch, the observed lines associated with the smallest and the largest rotational quantum number J'' were chosen. All values are in cm^{-1}

Band	Line	Exp.[c]	MP2[d]	B0	B0-1[e]	B0-2[e]	MSC_o[e]	BD_2	BQ_2	BQe_2	RMR[a]
(1,0)	P(28)	858.1	44.3	48.0	19.8	18.5	16.0	12.7	4.6	3.7	3.5
	P(1)	1344.9	35.9	45.2	14.3	13.8	11.7	9.3	2.8	2.0	1.9
	R(0)	1374.1	36.1	45.2	14.3	13.8	11.7	9.3	2.8	2.0	1.8
	R(22)	1550.1	49.0	54.2	20.5	19.2	16.4	12.9	3.8	2.8	2.5
(2,1)	P(27)	844.9	46.5	49.0	21.3	19.8	17.1	13.1	4.1	3.2	2.9
	P(1)	1300.5	38.5	33.5	14.5	13.8	11.4	9.1	1.6	0.8	0.6
	R(0)	1328.8	38.9	33.7	14.6	13.9	11.5	9.2	1.6	0.8	0.6
	R(17)	1485.9	47.8	44.1	19.4	18.0	15.2	11.8	2.3	1.4	1.1
(3,2)	P(23)	885.7	47.4	44.3	21.1	20.2	17.4	13.3	3.7	2.7	2.4
	P(1)	1256.9	42.1	36.3	17.0	15.5	12.9	9.9	1.4	0.5	0.3
	R(0)	1284.5	42.3	36.5	17.1	15.5	13.0	9.9	1.3	0.4	0.2
	R(18)	1439.4	53.5	47.8	22.5	21.3	18.1	13.8	2.7	1.5	1.2
(4,3)	P(21)	888.2	50.2	43.4	23.8	21.9	18.9	14.4	3.8	2.7	2.4
	P(2)	1200.3	46.1	38.8	19.5	18.1	15.3	11.5	1.8	0.9	0.6
	R(1)	1253.7	47.0	39.5	19.8	18.4	15.5	11.7	1.8	0.8	0.5
	R(14)	1373.1	54.9	45.5	24.5	22.5	19.2	14.6	2.8	1.7	1.3
(5,4)	P(15)	957.1	52.0	45.9	25.0	22.8	19.7	14.9	3.6	2.4	2.1
	P(3)	1144.9	50.6	42.4	22.8	21.1	18.1	13.6	2.6	1.5	1.2
	R(4)	1244.9	53.1	44.4	24.0	22.2	19.0	14.3	2.8	1.6	1.2
	R(8)	1283.8	55.5	46.8	25.5	23.5	20.1	15.2	3.0	1.8	1.5
(2,0)	P(25)	2109.9	92.5	99.1	40.8	38.1	32.8	25.5	8.2	6.3	5.8
	P(1)	2659.8	74.6	78.7	28.8	27.5	23.2	18.3	4.4	2.8	2.4
	R(1)	2701.6	75.1	79.1	29.0	27.8	23.4	18.5	4.4	2.8	2.5
	R(13)	2785.8	84.1	89.5	34.0	32.1	27.2	21.5	5.6	3.9	3.5
(3,1)	P(22)	2116.9	94.8	91.0	41.3	38.8	33.3	25.6	6.7	4.7	4.2
	P(1)	2571.4	80.7	69.9	31.5	29.3	24.4	19.0	2.9	1.3	0.9
	R(0)	2599.3	81.1	70.1	31.7	29.4	24.5	19.1	2.9	1.3	0.9
	R(11)	2689.0	88.5	78.6	35.4	33.1	27.8	21.6	3.8	2.0	1.5
(4,2)	P(19)	2118.4	98.9	87.1	44.1	41.3	35.4	26.9	6.4	4.3	3.7
	P(3)	2454.5	88.3	75.4	36.6	33.6	28.3	21.5	3.2	1.3	0.8
	R(1)	2524.2	89.2	75.9	36.9	33.9	28.5	21.7	3.1	1.3	0.7
	R(11)	2598.1	97.0	83.1	41.2	38.1	32.3	24.5	4.2	2.2	1.6
(5,3)	P(16)	2114.2	104.5	90.3	49.1	44.9	38.6	29.2	6.8	4.4	3.8
	P(2)	2385.4	97.3	81.6	42.5	39.4	33.5	25.3	4.5	2.3	1.7
	R(5)	2477.1	100.8	84.5	44.4	41.1	35.0	26.4	4.8	2.6	2.0
	R(13)	2511.6	109.9	93.7	50.6	46.4	39.8	30.0	6.3	3.8	3.2
(6,4)	P(11)	2145.4	109.9	101.4	53.3	48.6	42.0	31.6	7.3	4.6	4.0
	P(5)	2255.9	107.4	96.6	50.8	46.6	40.1	30.1	6.4	3.9	3.3

[a] From ref.[41] [b] From ref.[32] [c] From ref.[44] [d] Obtained from an 'unstable' local minimum of the PEC (see text). [e] See Table VI.

tions using the cc-pVQZ basis set with respect to that required by the BD_2 approximation ($T_r = 1.0$) leads to similar results: $T_r \approx 0.12$ for B0 and $T_r \approx 0.25$ for B0-1.

C. Application to the BeH Molecule

Next, we apply the B0 approximations to the simple open-shell system, the ground state $X^2\Sigma^+$ of the BeH molecule, which represents a natural extension of the preceding molecule LiH. Hence, we have to use a restricted open-shell Hartree–Fock (ROHF) wave function as a reference and we also employ the cc-pV(D,T,Q)Z basis sets. In this case it is well known (cf. f) of ref.[11] and refs[45,46]) that the ROHF solution for BeH is plagued with doublet instabilities which is caused by a qualitative change in the bounding nature when stretching the BeH bound from equilibrium geometry to the dissociation-limit: at the equilibrium geometry a 1s electron participates in the σ-bond (closed-shell), whereas in the case of separated atoms we have the closed-shell Be atom and open-shell electron on the H atom. Therefore, in order to obtain a smooth PEC, we start the calculation at the stretched geometry (9 a.u.), based on the so-called outer ROHF solution[11,46].

Here, it should be stated that for BeH only one (ROHF) determinant reference function (1D SR) is used. Now, we consider first the 1D SR results of the spectroscopic constants for MP2 and various DGB approaches given in Table X. The results of the advanced approximations, BD_2 to FCI (if available), are given for comparison with the B0-based approaches. As these results show, all of these "advanced" methods lead to similar results for each of the basis set employed. Comparing these values with the experimental results shown in Table X we obtain a relatively good agreement if we are focusing on the cc-pV(D,Q)Z basis sets. The cc-pVTZ basis set shows slightly deteriorated values for anharmonic parts of the spectroscopic constants compared with the behavior of the cc-pV(D,Q)Z bases. Here, the results of BQ_4 are close to the FCI results in the case of the cc-pVDZ basis set, which indicate, as shown earlier for LiH, that the FCI results for the cc-pVTZ basis set should be similar to the values of BQ_4. Next, we proceed with the B0 and MP2 results of Table X. The approximated values of the spectroscopic constants at the equilibrium geometry R_e and ω_e obtained with cc-pVDZ are in good agreement with the FCI values, which holds also for the B_e and $\mathbf{D}_e$ constants. However, if we consider the anharmonic constants, here the MP2 values suite better to the FCI and experimental results than does B0. For the dissociation energy D_e, B0 gives the closer estimate with respect to the FCI result. If we employ the cc-pVTZ basis set, the data of the B0 ap-

TABLE X

Experimental results and computed spectroscopic constants (in cm^{-1}, μ_e in D, R_e in Å) for the BeH molecule, obtained with different approximations using different correlated basis sets (the numbers in parentheses give the exponents in base 10)

Method	Basis set[a]	$-\mu_e$	D_e	R_e	ω_e	$\omega_e x_e$	B_e	α_e	D_e
B0	cc-pVDZ	0.209	15112.7	1.3598	2051.66	23.02	10.0570	0.1885	0.9711(–3)
	cc-pVTZ	0.249	17106.7	1.3270	2248.90	154.87	10.5614	0.4143	1.0272(–3)
	cc-pVQZ	0.228	17349.7	1.3364	2035.72	0.73	10.4123	0.3509	1.0497(–3)
MP2	cc-pVDZ	0.203	17976.5	1.3531	2091.21	31.97	10.1583	0.2657	0.9588(–3)
	cc-pVTZ	0.223	19310.8	1.3274	2113.76	37.78	10.5548	0.3406	1.0521(–3)
	cc-pVQZ	0.247	19422.1	1.3361	2112.31	34.61	10.4178	0.2835	1.0145(–3)
B0[D_2,–]	cc-pVDZ	0.203	16264.5	1.3525	2081.17	29.69	10.1667	0.2633	0.9693(–3)
	cc-pVTZ	0.227	18114.8	1.3264	2133.95	58.34	10.5713	0.3547	1.0564(–3)
	cc-pVQZ	0.242	18439.0	1.3353	2109.64	34.10	10.4304	0.2908	1.0201(–3)
B0[–,D_2]	cc-pVDZ	0.203	16320.3	1.3524	2081.80	29.70	10.1680	0.2636	0.9690(–3)
	cc-pVTZ	0.228	18176.5	1.3263	2134.11	57.88	10.5722	0.3538	1.0562(–3)
	cc-pVQZ	0.242	18494.4	1.3352	2109.57	33.58	10.4320	0.2908	1.0202(–3)
B0[D_2,D_2]	cc-pVDZ	0.161	15841.8	1.3548	2063.59	32.59	10.1327	0.2793	0.9756(–3)
	cc-pVTZ	0.212	17579.0	1.3290	2093.24	43.77	10.5285	0.3573	1.0693(–3)
	cc-pVQZ	0.266	17930.9	1.3378	2097.25	38.32	10.3914	0.2940	1.0237(–3)
MSC_o[b]	cc-pVDZ	0.198	15496.8	1.3553	2059.01	33.09	10.1242	0.2813	0.9774(–3)
	cc-pVTZ	0.209	17637.9	1.3297	2087.62	44.63	10.5184	0.3610	1.0721(–3)
	cc-pVQZ	0.228	18339.6	1.3387	2090.08	38.86	10.3768	0.2973	1.0263(–3)
BD_2	cc-pVDZ	0.185	15854.2	1.3555	2059.01	35.83	10.1211	0.2850	0.9780(–3)
	cc-pVTZ	0.211	17531.1	1.3298	2079.67	38.96	10.5170	0.3588	1.0740(–3)
	cc-pVQZ	0.237	17877.4	1.3384	2089.35	36.78	10.3817	0.2950	1.0265(–3)
BQ_2	cc-pVDZ	0.185	15849.9	1.3557	2057.84	35.99	10.1190	0.2855	0.9785(–3)
	cc-pVTZ	0.209	17410.4	1.3301	2075.26	39.96	10.5115	0.3634	1.0770(–3)
	cc-pVQZ	0.234	17582.8	1.3398	2075.81	36.15	10.3598	0.3012	1.0315(–3)
BQe_2	cc-pVDZ	0.184	15854.7	1.3558	2056.92	36.27	10.1169	0.2859	0.9788(–3)
	cc-pVTZ	0.208	17405.8	1.3302	2073.75	39.94	10.5095	0.3639	1.0778(–3)
	cc-pVQZ	0.233	17569.0	1.3401	2076.72	38.12	10.3555	0.3008	1.0310(–3)
BQ_4	cc-pVDZ	0.178	15979.1	1.3575	2044.70	36.71	10.0917	0.2889	0.9828(–3)
	cc-pVTZ	0.205	17526.8	1.3315	2066.27	43.02	10.4903	0.3702	1.0817(–3)
	cc-pVQZ	–	–	–	–	–	–	–	–
FCI	cc-pVDZ	0.178	15984.3	1.3575	2044.77	37.33	10.0911	0.2909	0.9828(–3)
	cc-pVTZ	–	–	–	–	–	–	–	–
	cc-pVQZ	–	–	–	–	–	–	–	–
Exp.[c]			18550.6	1.3426	2060.78	36.31	10.3164	0.3030	1.0221(–3)

[a] From ref.[32] [b] From refs[26,37], D_e from ref.[39] [c] Here, MSC_o stands for B0[D_2,D_2]msc (see text).

proach unfortunately deteriorate except for D_e (and μ_e, here, with respect to BQe_2). This also holds for the MP2 results but not so extremely as in the case of the B0 approach. This can be slightly remedied by augmenting the basis set to cc-pVQZ. Nevertheless, the results are still worser in the case of the anharmonic constants $\omega_e x_e$ and α_e for B0 than for MP2 in contrast to the results of D_e (and μ_e with respect to BQe_2). The deteriorating behavior of the results of the spectroscopic constants, especially for $\omega_e x_e$ and α_e, using the cc-pVTZ basis set, can also be seen in the results of the advanced DGB approaches.

In order to improve or remedy the behavior of the B0 approach by low computational cost, Table X presents also the results of the internal-corrected B0 approximations, namely B0[D_2,–], B0[–,D_2], and B0[D_2,D_2] as well as the B0[D_2,D_2]-based size-extensivity correction of Molnar and Szalay (MSC_o, cf. Eq. (*19*)). In Fig. 4, we present the ground state $X^2\Sigma^+$ PECs of the B0 and B0[D_2,D_2] approximations and also those obtained by the MP2 and FCI methods. As in the case of LiH, we observe at least in this case of a small molecule that the results (given in Table X) of the internal-corrected methods – be the correction applied during the iteration of B0, namely B0[D_2,–], or at the end, namely B0[–,D_2] – are quite similar (but improved). Thus, we can expect a further (slight) improvement if we apply the B0[D_2,D_2] approximation to the ground state of BeH as shown in Table X. That also holds if we use in addition the Molnar and Szalay correction, i.e. MSC_o. The percentage of the relative deviation of the latter approach (obtained with the cc-pVQZ basis set) by considering the experimental values is below 2% except for the anharmonic constant $\omega_e x_e$ (about 7%) and the dipole moment μ_e (about 2.1% with respect to the BQe_2 results). The relative computational time of the B0 and B0[D_2,D_2] approximations using the cc-pVQZ basis set with respect to that required by the BD_2 approximation (T_r = 1.0) leads here to similar results as in the case of LiH: $T_r \approx 0.10$ for B0 and $T_r \approx 0.25$ for B0[D_2,D_2].

Following the LiH presentation, Table XI and Table XII show the results of the vibrational energy levels (first part), the fundamental vibrational transition energies (second part), and transition frequencies for selected lines in the P and R branches of vibrational bands (last part). In the case of Table XI, these data are obtained with the cc-pVDZ basis set whereas Table XII presents the values generated with the cc-pVQZ basis set. As before, we show the deviation results of the B0-based approximations (B0, B0[D_2,D_2], i.e. B0-1, and MSC_o), of the MP2 and advanced DGB approaches (BD_2, BQ_2, and BQe_2) with respect to the available FCI values also given in Table XI. First of all we recognize that the results of the B0 method lead to better

agreement with the FCI values than does MP2. Moreover, we have the same behavior of the B0-based methods as in the case of LiH: B0, B0-1, and MSC_o. The substantial improvement is obtained with the incorporation of the internal corrections based on the BD_2 approach (B0-1). In addition MSC_o leads to small corrections for the low-lying vibrational energy levels ν and with increasing levels ν we obtain better correction. Similar behavior can be found in the case of the fundamental vibrational transition energies. The third part of data given in Table XI, the transition frequencies show also substantial improvement with the incorporation of the internal corrections based on the BD_2 approach (B0-1) and, moreover, further (smaller) corrections can also be obtained with the MSC_o approach. When considering the results obtained with the cc-pVQZ basis set presented in Table XII,

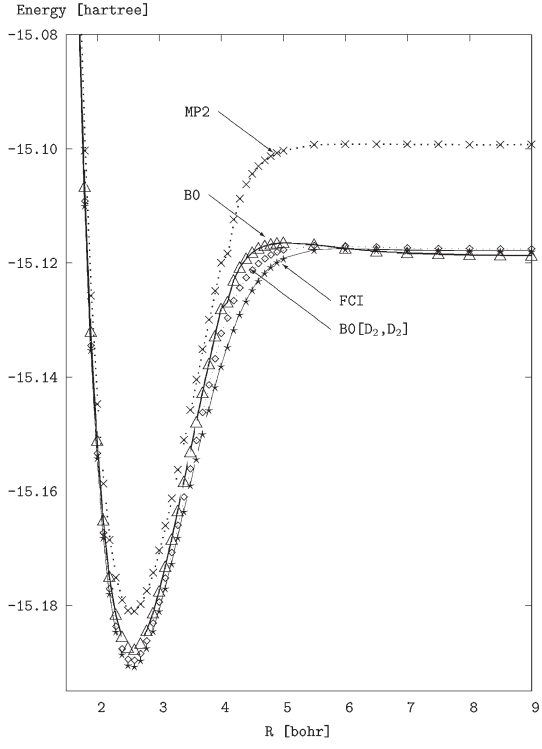

FIG. 4
Potential energy curves for the BeH ground state, obtained with the MP2, B0, B0[D_2,D_2], and FCI approximations and the cc-pVDZ basis set

TABLE XI

First part, FCI vibrational energy levels[a] of BeH and the differences between MP2, various DGB computed values and the FCI results. Second part, the fundamental ($v \rightarrow v + 1$) vibrational transition energies (FCI) of BeH and the deviations of the computed values from FCI. Third part, the deviations of the transition frequencies of the approximations from the FCI values for selected lines in the P and R branches of various vibrational bands of BeH. All values are in cm^{-1} and obtained with the cc-pVDZ basis[b]

v	MP2	B0	B0-1[c]	MSC_o[d]	BD_2	BQ_2	BQe_2	FCI[a]
0	14.0	11.5	5.1	4.0	3.2	2.9	2.6	995.1
1	71.9	45.8	32.5	25.8	20.7	18.8	17.1	2964.8
2	143.4	105.0	68.4	54.6	42.1	38.3	34.5	4857.8
3	231.6	185.3	114.2	91.5	68.8	62.2	55.5	6670.7
4	341.1	282.3	173.7	139.4	102.6	92.1	81.2	8398.5
5	477.5	400.1	251.3	201.5	145.2	129.1	111.9	10033.6
6	646.2	541.5	349.9	275.0	191.3	166.1	140.9	11564.4
7	840.9	675.8	449.4	318.3	199.6	159.6	133.6	12973.0
8	1051.7	698.2	474.8	266.7	138.5	92.5	79.2	14229.1
9	1355.7	–	375.2	168.7	103.8	68.6	57.1	15277.6
10	1674.4	–	–	–	–	–	–	15981.1

v	MP2	B0	B0-1[c]	MSC_o[d]	BD_2	BQ_2	BQe_2	FCI[a]
0	57.9	34.3	27.5	21.8	17.5	16.0	14.5	1969.7
1	71.5	59.2	35.8	28.8	21.4	19.4	17.4	1893.0
2	88.2	80.3	45.9	36.9	26.7	24.0	21.0	1812.9
3	109.4	97.0	59.4	47.9	33.8	29.9	25.6	1727.8
4	136.5	117.8	77.6	62.1	42.7	37.0	30.7	1635.1
5	168.7	141.4	98.6	73.4	46.1	36.9	29.0	1530.9
6	194.7	134.3	99.5	43.3	8.3	–6.5	–7.3	1408.6
7	210.8	22.4	25.4	–51.6	–61.2	–67.1	–54.3	1256.2
8	303.9	–	–99.5	–98.0	–34.6	–23.9	–22.1	1049.0
9	318.7	–	–	–	–	–	–	703.5

TABLE XI
(*Continued*)

Line	MP2	B0	B0-1[c]	MSC_o[d]	BD_2	BQ_2	BQe_2	FCI[a]
(1,0)								
R(2)	58.81	35.29	27.96	22.19	17.78	16.23	14.76	2025.71
R(1)	58.45	34.83	27.76	22.03	17.66	16.12	14.66	2007.69
R(0)	58.15	34.51	27.59	21.89	17.55	16.03	14.57	1989.03
P(1)	57.75	34.32	27.36	21.71	17.40	15.89	14.44	1949.85
P(2)	57.66	34.43	27.30	21.66	17.35	15.84	14.40	1929.39
(2,1)								
R(2)	72.66	60.17	36.52	29.34	21.84	19.80	17.71	1947.08
R(1)	72.17	59.74	36.25	29.12	21.68	19.66	17.58	1929.71
R(0)	71.77	59.41	36.03	28.94	21.55	19.53	17.47	1911.67
P(1)	71.22	58.98	35.72	28.69	21.35	19.35	17.31	1873.72
P(2)	71.08	58.89	35.63	28.62	21.29	19.30	17.26	1853.84
(2,0)								
R(2)	130.78	94.94	64.09	51.21	39.36	35.80	32.25	3915.03
R(1)	130.15	94.23	63.74	50.93	39.17	35.62	32.09	3898.85
R(0)	129.68	93.75	63.48	50.72	39.01	35.48	31.97	3881.42
P(1)	129.21	93.47	63.21	50.50	38.84	35.32	31.83	3842.86
P(2)	129.20	93.67	63.19	50.49	38.81	35.30	31.80	3821.79

[a] Obtained with GAMESS [31]. [b] From ref.[32]. [c] Here, B0-1 stands for B0[D_2,D_2] (see text). [d] Here, MSC_o stands for B0[D_2,D_2]msc (see text).

we have a similar situation for B0 and MP2 as in the case of the cc-pVDZ basis set. However, the B0 approach leads to much better results compared with the MP2 results by using BQe_2 as reference method. Unfortunately, if we apply the internal correction to B0, namely B0-1, here we do not obtain a significant refinement of the data. That holds also for the MSC_o approximation. Here, it seems that these relatively good results of the B0 approach and the ill-conditioned B0-1 and MSC_o approaches are an expression of the PEC and the spectroscopic constant, respectively, given in Table X, especially considering the anharmonic part $\omega_e x_e$.

TABLE XII

First part, BQe_2 vibrational energy levels of BeH and the differences between MP2, other DGB computed values and the BQe_2 results. Second part, the fundamental ($v \rightarrow v + 1$) vibrational transition energies of BeH and the deviations from BQe_2. Third part, the deviations of the transition frequencies of the approximations from the BQe_2 values for selected lines in the P and R branches of various vibrational bands of BeH. All values are in cm^{-1} and obtained with the cc-pVQZ basis[a]

v	MP2	B0	B0-1[b]	MSC_o[c]	BD_2	BQ_2	BQe_2
0	26.0	11.3	13.8	8.4	9.9	1.3	1011.9
1	68.7	17.3	36.1	22.2	25.5	2.9	3013.4
2	119.3	39.3	63.4	39.5	44.8	5.7	4940.7
3	179.0	73.3	98.7	63.0	68.9	9.2	6793.4
4	250.2	144.4	144.0	94.8	99.2	14.8	8569.6
5	336.6	213.7	199.6	138.8	135.9	22.3	10265.5
6	447.8	293.9	259.0	214.2	168.0	33.7	11875.2
7	611.2	348.9	307.6	364.2	176.5	51.1	13388.6
8	865.8	415.2	412.1	592.4	237.3	79.4	14788.6
9	1189.1	601.4	629.7	638.3	378.5	123.2	16029.7
10	1463.3	503.0	595.6	563.5	357.8	105.1	16940.8
11	1727.5	–	–	–	–	–	17485.2

v	MP2	B0	B0-1[b]	MSC_o[c]	BD_2	BQ_2	BQe_2
0	42.7	5.9	22.3	13.8	15.6	1.7	2001.5
1	50.6	22.1	27.3	17.3	19.3	2.7	1927.3
2	59.8	34.0	35.2	23.5	24.1	3.6	1852.7
3	71.2	71.1	45.3	31.8	30.3	5.6	1776.2
4	86.3	69.3	55.7	44.0	36.7	7.5	1696.0
5	111.2	80.1	59.3	75.4	32.1	11.4	1609.6
6	163.4	55.1	48.6	149.9	8.5	17.4	1513.4
7	254.6	66.3	104.5	228.2	60.8	28.3	1399.9
8	323.4	186.2	217.6	46.0	141.2	43.7	1241.1
9	274.1	–98.4	–34.0	–74.8	–20.8	–18.0	911.1
10	264.2	–	–	–	–	–61.8	544.4

TABLE XII
(*Continued*)

Line	MP2	B0	B0-1[b]	MSC_o[c]	BD_2	BQ_2	BQe_2
(1,0)							
R(2)	43.42	5.97	22.64	14.04	15.87	1.69	2059.01
R(1)	43.14	5.98	22.49	13.95	15.76	1.67	2040.50
R(0)	42.91	5.97	22.36	13.87	15.67	1.66	2021.33
P(1)	42.58	5.85	22.18	13.76	15.53	1.64	1981.13
P(2)	42.48	5.75	22.12	13.73	15.49	1.64	1960.14
(2,1)							
R(2)	51.42	22.43	27.85	17.67	19.65	2.77	1982.94
R(1)	51.08	22.26	27.64	17.52	19.50	2.75	1965.04
R(0)	50.79	22.13	27.47	17.42	19.38	2.73	1946.49
P(1)	50.37	22.00	27.23	17.27	19.20	2.71	1907.50
P(2)	50.23	22.00	27.16	17.23	19.15	2.70	1887.12
(2,0)							
R(2)	94.28	28.27	50.19	31.53	35.29	4.43	3982.66
R(1)	93.85	28.16	49.93	31.35	35.11	4.41	3965.98
R(0)	93.52	28.06	49.73	31.22	34.97	4.39	3948.03
P(1)	93.14	27.91	49.51	31.09	34.82	4.37	3908.43
P(2)	93.09	27.85	49.49	31.08	34.80	4.36	3886.84

[a] From ref.[32] [b] Here, B0-1 stands for $B0[D_2,D_2]$ (see text). [c] Here, MSC_o stands for $B0[D_2,D_2]$msc (see text).

D. Application to the Phenolate Anion

As an initial assessment of the B0 approach in the case of larger molecular systems, we here calculate the energies of the ground and excited states of the phenolate anion. The geometry of the isolated anion is taken from ref.[12] where the optimized geometry has been determined using restricted Hartree–Fock (RHF) calculations, the standard 4-31G basis set[31], and C_s symmetry. Therefore, all the calculations are based on the 4-31G basis set. In order to asses the B0 approach we compare the B0 results with other calculations of ref.[12], such as the first, second, and third order of the effective

valence shell Hamiltonian (H^v) method by using improved virtual orbitals (IVOs), the equation-of-motion coupled-cluster method with restriction to all single and double excitations (EOM-CCSD), the state-average complete active space SCF (sa-CASSCF) method and its second-oder correlation correction extension (sa-CASMP2), and the single-excitation configuration interaction (CIS) approach (for details of these methods we refer to ref.[12] and references therein). Moreover, a full configuration interaction calculation[31] has been performed within a selected active space (SAS-FCI) containing eight electrons and 12 orbitals: four double occupied orbitals (2π,3π,21σ,4π) and eight unoccupied orbitals in the ground state configuration:

$$[(2\pi)^2\ (3\pi)^2\ (21\sigma)^2\ (4\pi)^2]\ \{(5\pi)(6\pi)(22\sigma)\ \ldots\ (26\sigma)(7\pi)\}\ .$$

The results of the SAS-FCI calculation have been used to classify the excited states and therefore the dominant determinants of the state functions which are then used in our calculation: a single reference determinant in the case of triplet and quintet states and a two-determinant reference function in the case of singlet states. The results of the energy calculations are presented in Table XIII. Here, Table XIII shows the excitation energies (in eV) of the first fourteen singlet (S_i) and triplet (T_i) states, and one quintet (Q_1) state of the isolated phenolate anion obtained with various calculation methods mentioned above. The first column shows the order of the single, triplet, and quintet states obtained with the SAS-FCI computation (see third column of Table XIII). The second column presents the excitation scheme of the dominant configuration used with respect to the ground state configuration.

Here, it should be stressed that the H^v calculation is performed within a valence reference space containing the first seven π-orbitals (1π, ..., 7π). Then the effective valence shell Hamiltonian is diagonalized solely within this reference space to yield all reference space states energies. It means that only excitations of $\pi \rightarrow \pi$ type are considered in ref.[12] (see Table 2 therein) and presented in Table XIII. Although the assignment of the states of the H^v calculation, shown in Table 2 of ref.[12], to the states of the SAS-FCI calculation are not unambiguously for all states, we arrange the ambiguous states, here S_8, S_{11}, and S_{13}, by the order of the excitation energies of the B0 results.

Comparing the SAS-FCI and the B0 excitation energies we can find good correspondence in the order of the states with the exceptions of the singlet states S_6, S_8, S_{11}, and S_{13}. For the S_{11} and S_{13} states B0 leads to lower excitation energies than does SAS-FCI ($\Delta(S_{11}) \approx -1.152$ eV, $\Delta(S_{13}) \approx -0.721$ eV), in

TABLE XIII

Comparison of excitation energies (in eV) for the isolated phenolate anion obtained with various approximations using the 4-31G basis set[a]

States	Configuration	SAS-FCI[a]	B0	$H^{v\ b}_{1st}$	$H^{v\ b}_{2nd}$	$H^{v\ b}_{3rd}$	CCSD[b]	CASSCF[b]	CASMP2[b]	CIS[b]
T_1	$(4\pi\rightarrow5\pi)$	4.080	3.757	3.983	3.498	3.688	3.611	3.580	3.692	3.671
T_2	$(4\pi\rightarrow6\pi)$	4.271	4.234	4.087	4.109	3.933	3.871	3.830	3.945	3.765
S_1	$(4\pi\rightarrow5\pi)$	4.986	4.853	4.686	4.202	4.391	4.419	4.288	4.395	5.476
T_3	$(3\pi\rightarrow5\pi)$	5.285	5.338	4.954	5.409	4.948	5.002	4.894	4.990	4.646
T_4	$(21\sigma\rightarrow5\pi)$	5.998	5.441							
S_2	$(21\sigma\rightarrow5\pi)$	6.129	5.562							
T_5	$(21\sigma\rightarrow6\pi)$	6.157	5.600							
S_3	$(21\sigma\rightarrow6\pi)$	6.269	5.749							
S_4	$(4\pi\rightarrow6\pi)$	6.525	6.015	6.197	5.800	5.656	5.761	6.037	6.111	6.412
T_6	$(4\pi\rightarrow22\sigma)$	6.769	6.633							
S_5	$(4\pi\rightarrow22\sigma)$	6.864	6.720							
T_7	$(3\pi\rightarrow6\pi)$	7.396	7.311	6.754	7.111	6.525				
T_8	$(2\pi\rightarrow6\pi)$	7.861	8.071	7.450	7.664	7.191				
T_9	$(2\pi\rightarrow5\pi)$	7.905	8.172	7.705	7.448	7.269				
S_6	$(3\pi\rightarrow6\pi)$	8.091	8.001	7.543	7.535	7.122	7.497	7.303	7.428	
T_{10}	$(4\pi\rightarrow23\sigma)$	8.255	8.163							
S_7	$(4\pi\rightarrow23\sigma)$	8.299	8.176							
S_8	$(4\pi^2\rightarrow5\pi^2)$	8.450	9.951	9.009	8.331	8.229				
T_{11}	$(21\sigma\rightarrow22\sigma)$	8.504	8.351							
S_9	$(21\sigma\rightarrow22\sigma)$	8.587	8.436							
T_{12}	$(4\pi\rightarrow24\sigma)$	8.680	8.643							
S_{10}	$(4\pi\rightarrow24\sigma)$	8.871	8.835							
Q_1	$(3,4\pi\rightarrow5,6\pi)$	8.903	8.814	8.654	9.128	8.501				
S_{11}	$(3\pi\rightarrow5\pi)$	9.017	7.865	7.890	7.508	7.350				
T_{13}	$(3\pi\rightarrow22\sigma)$	9.073	8.949							
S_{12}	$(3\pi\rightarrow22\sigma)$	9.227	9.082							
S_{13}	$(2\pi\rightarrow5\pi)$	9.488	8.767	8.640	8.363	8.022				
T_{14}	$(4\pi\rightarrow25\sigma)$	9.574	9.261							
S_{14}	$(4\pi\rightarrow25\sigma)$	9.644	9.383							

[a] Ref.[31] (see text). [b] From ref.[12], where CCSD ≡ EOM-CCSD, CASSCF ≡ sa-CASSCF, CASMP2 ≡ sa-CASMP2.

contrast to the S_8 state where the B0 calculation delivers a much higher excitation energy ($\Delta(S_8)$ = 1.501 eV). Differences of the other states vary from –0.567 to 0.267 eV. To determine the order of the singlet states S_6, S_8, S_{11}, and S_{13} we compare the B0 results with the excitation energies of the H^v calculations. Here the first order results, H^v_{1st}, of the S_{11} and S_{13} singlet states agree with the B0 results within 0.13 eV whereas the S_6 and S_8 states differ by 0.458 and 0.942 eV, respectively. With respect to the H^v calculation we obtain for B0 an average deviation of 0.227 eV in the case of the first order, of about 0.340 eV in the case of the second order, and finally 0.572 eV in the case of the third oder of H^v if we exclude the double excited singlet state S_8. For that case and with respect to the EOM-CCSD results the differences for the B0 approach vary now from 0.146 eV for the first triplet state T_1 to 0.504 eV for the singlet state S_6 which leads to an average deviation of 0.340 eV. Additionally, the sa-CASSSCF and the sa-CASPT2 results are also in good agreement with the results of the EOM-CCSD method, where the sa-CASMP2 excitation energies are higher than the corresponding sa-CASSCF values for all states shown. However, considering the results of the CIS calculation the singlet states S_1 and S_4 are much higher than the results of the other approaches except SAS-FCI. Thus, except for the S_8 states the comparison shows a good agreement in the order of the states and of the excitation energies of the B0 method with the H^v and the EOM-CCSD results. Here, the poor performance of the B0 approach for the S_8 states results from the multiconfiguration character which should comprise at least five determinants in contrast to the two determinant-ansatz for the reference function in the case of the B0 approximation.

The results of Table XIII illustrates that the B0 approach suffices to treat the singlet and triplet states for the isolated phenolate anion. Moreover, it also illustrates the limitation of the two-determinant reference-state ansatz. Here, it should also be emphasized that a calculation of the correlation energy for each state comprise about two third of the calculation whereas the SCF part covers the first third of the calculation (SCF: ≈25 s/B0: ≈50 s).

IV. CONCLUSION

In this paper we explored the efficiency and reliability of the direct iterative approach to the solution of the generalized Bloch equation at the computational most efficient level, the B0 approach and B0-based approaches as well. Since we are interested in methods which can be easily extended and applied to large molecular systems, the B0 approach seems to be an efficiency and reliability candidate for that purpose. In order to test the reli-

ability of the B0 approaches, we compare these B0 approximations with experimental data, if available, and approaches with and without relying on the exponential cluster expansion ansatz.

For the purpose of assessment of the B0 and B0-based approaches in the case of the Li and Be atoms, we determine the energies of the ground states and the excited states as well as the polarizabilities α and γ of Li. Whereas, in the case of LiH and BeH, we calculate the PECs of the ground state in the range of the internuclear separation from 1 to about 15 a.u. obtained with cc-pV(D,T,Q)Z basis sets for the determination of the spectroscopic coefficients and the vibrational levels. Furthermore, dissociation energies and the dipole moments of the equilibrium geometry have been calculated. Then the results are compared with MP2 and other higher level DGB, CI, and CC methods as well as with FCI and experimental results (if available). For the phenolate anion we use the 4-31G basis set at a optimized geometry to calculate the excitation energies. Here, we compare the B0 results with the effective valence shell Hamiltonian (H^v) method, the EOM-CCSD, CASSCF, CASMP2, and CIS approach.

The analysis of these calculations leads to the following conclusion: Taking into account the simplicity and the computational low requirement of the B0 approximations, we obtain a qualitative and in some cases also quantitative good agreement with the benchmark FCI results and even with the experimental results if we systematically improve the method proceeding from the very affordable, low-level B0 to a low-level internal correction, as well as to size-extensive corrections on top which are usually based on the CISD approximation. Here, it should be emphasized that the B0 approach leads in some cases to similar results, e.g. for spectroscopic constants, as MP2 at the equilibrium geometry. However, B0 provides a much better behavior considering stretched internuclear separation. The B0 method does not suffer of the divergent behavior as MP2. Also in the case of the vertical excitation energies for the phenolate anion the B0 approach leads to sufficient results by low computational cost compared e.g. with the results of the low-lying states of the EOM-CCSD, and even if we compare the results with the widely used CIS approach. The B0 approach suffices to treat the low-lying singlet and triplet states for the isolated phenolate anion.

It means that the approximations employed in this paper, namely B0 and the B0-based corrections – be it the internal correction or the size-extensivity correction – may not be suitable when high accuracy is required. However, these approaches seem to be useful when reasonable results are

asked for medium-sized or large systems by low computational cost where no methods of chemical accuracy are available.

The author would like to thank Prof. J. Paldus and Dr. X. Li for valuable and helpful discussions, and acknowledge the support of Prof. B. Dick of the Department of Chemistry and the staff of the Computer Center at the University of Regensburg. Moreover, the author wishes to thank Prof. J. Paldus and the Department of Applied Mathematics of the University of Waterloo for their hospitality.

REFERENCES

1. Langhoff S. R. (Ed.): *Quantum Mechanical Electronic Structure Calculations with Chemical Accuracy*. Kluwer Academic, Dordrecht Netherlands 1995; and references therein.
2. Bartlett R. J. in: *Modern Electronic Structure Theory*, Part I (D. R. Yarkony, Ed.), p. 1047. World Scientific, Singapore 1995.
3. Bartlett R. J. (Ed.): *Recent Advances in Computational Chemistry*, Vol. 3. World Scientific, Singapore 1997.
4. a) Paldus J., Li X.: *Adv. Chem. Phys.* **1999**, *110*, 1; b) Paldus J. in: *Handbook of Molecular Physics and Quantum Chemistry* (S. Wilson, Ed.), Vol. 2, Part 3, Chap. 19, p. 272. J. Wiley, Chichester 2003.
5. Piecuch P., Kowalski K. in: *Computational Chemistry: Reviews of Current Trends* (J. Leszcynski, Ed.), Vol. 5, p. 1. World Scientific, Singapore 2000.
6. a) Lindgren I.: *Int. J. Quantum Chem., Quantum Chem. Symp.* **1978**, *12*, 33; b) Lindren I., Morrison J. (Eds): *Atomic Many-Body Theory*, 2nd ed. Springer Verlag, Berlin 1986; c) Lindgren I., Mukherjee D.: *Phys. Rep.* **1987**, *151*, 93; d) Mukherjee D., Pal S.: *Adv. Quantum Chem.* **1989**, *20*, 292.
7. Jeziorski B., Monkhorst H. J.: *Phys. Rev. A* **1981**, *24*, 1668.
8. Li X., Paldus J.: *J. Chem. Phys.* **2004**, *120*, 5890; and references therein.
9. Li X., Paldus J.: *J. Chem. Phys.* **2001**, *115*, 5759.
10. a) Piecuch P., Kondo A. E., Špirko V., Paldus J.: *J. Chem. Phys.* **1996**, *104*, 4699; b) Meissner H., Paldus J.: *Int. J. Quantum Chem.* **2000**, *80*, 782.
11. a) Meissner H., Steinborn E. O.: *Int. J. Quantum Chem.* **1997**, *63*, 257; b) Meissner H., Steinborn E. O.: *J. Mol. Struct. (THEOCHEM)* **1998**, *433*, 119; c) Meissner H., Paldus J.: *Int. J. Quantum Chem.* **2000**, *80*, 782; d) Meissner H., Paldus J.: *J. Chem. Phys.* **2000**, *113*, 2594; e) Meissner H., Paldus J.: *J. Chem. Phys.* **2000**, *113*, 2612; f) Meissner H., Paldus J.: *J. Chem. Phys.* **2000**, *113*, 2622; g) Meissner H., Ema I.: *J. Mol. Struct. (THEOCHEM)* **2001**, *547*, 171; h) Meissner H., Paldus J.: *Collect. Czech. Chem. Commun.* **2001**, *66*, 1164; i) Meissner H.: *J. Chem. Phys.* **2003**, *119*, 4126.
12. He Z., Martin Ch. H., Birge R., Freed K. F.: *J. Phys. Chem. A* **2000**, *104*, 2939.
13. Paldus J. in: *Relativistic and Electron Correlation Effects in Molecules and Solids*, Vol. 318, NATO Advanced Study Institute, Series B: Physics (G. L. Malli, Ed.), p. 207. Plenum Press, New York 1994.
14. Paldus J., Planelles J.: *Theor. Chim. Acta* **1994**, *89*, 13.
15. a) Li X., Paldus J.: *J. Chem. Phys.* **1997**, *107*, 6257; b) Li X., Paldus J.: *J. Chem. Phys.* **1998**, *108*, 637; c) Li X., Paldus J.: *J. Chem. Phys.* **1999**, *110*, 2844; d) Li X., Paldus J.: *Int. J. Quantum Chem.* **2000**, *77*, 281.
16. Peris G., Planelles J., Malrieu J.-P., Paldus J.: *J. Chem. Phys.* **1999**, *110*, 11708.

17. Flocke N., Schmalz T. G.: *Int. J. Quantum Chem.* **2000**, *76*, 83.
18. Davidson E. R.: *The World of Quantum Chemistry*. Reidel, Dordrecht 1974.
19. Langhoff R., Davidson E. R.: *Int. J. Quantum Chem.* **1974**, *8*, 61.
20. Brueckner K. A.: *Phys. Rev.* **1955**, *100*, 36.
21. Davidson E. R., Silver D. W.: *Chem. Phys. Lett.* **1977**, *52*, 403.
22. Pople J. A., Seeger R., Krishnan R.: *Int. J. Quantum Chem., Quantum Chem. Symp.* **1977**, *11*, 149.
23. Duch W., Diercksen G. H. F.: *J. Chem. Phys.* **1994**, *101*, 3018.
24. Meissner L.: *Chem. Phys. Lett.* **1988**, *146*, 204.
25. Fuesti-Molnar L., Szalay P. G.: *J. Phys. Chem.* **1996**, *100*, 6288.
26. Herzberg G.: *Molecular Spectra and Molecular Structure,* I. Diatomic Molecules, p. 66. Van Nostrand, New York 1959.
27. Hurley A. C.: *Introduction to Electron Theory of Small Molecules*, p. 6. Academic Press, London 1976.
28. Level 6.1; LeRoy R. J.: *A Computer Program Solving the Radial Schrödinger Equation for Bound and Quasibound Levels, and Calculating Various Expectation Values and Matrix Elements*. University of Waterloo Chemical Physics Research Report CP-555R, Waterloo, Ontario, Canada 1996.
29. Cohen H. D., Roothaan C. C. J.: *J. Chem. Phys.* **1965**, *43*, S34.
30. Kurtz H. A., Stewart J. J. P., Dieter K. M.: *J. Comput. Chem.* **1990**, *11*, 82.
31. Gamess; Schmidt M. W., Baldridge K. K., Boatz J. A., Elbert S. T., Gordon M. S., Jensen J. H., Koseki S., Matsunaga N., Nguyen K. A., Su S., Windus T. L., Dupuis M., Montgomery J. A., Jr.: *J. Comput. Chem.* **1993**, *14*, 1347.
32. a) Basis sets were obtained from the Extensible Computational Chemistry Environment Basis Set Database, Version 02/25/04, as developed and distributed by the Molecular Science Computing Facility, Environmental and Molecular Sciences Laboratory which is part of the Pacific Northwest Laboratory, P.O. Box 999, Richland, WA 99352, U.S.A., and funded by the U.S. Department of Energy. The Pacific Northwest Laboratory is a multi-program laboratory operated by Battelle Memorial Institute for the U.S. Department of Energy under contract DE-AC06-76RLO 1830. Contact David Feller or Karen Schuchardt for further information: *Theor. Chim. Acta* **1994**, *89*, 13; b) Dunning T. H., Jr.: *J. Chem. Phys.* **1989**, *90*, 1007.
33. Paldus J., Li X.: *Can. J. Chem.* **1996**, *74*, 918.
34. Molof R. W., Schwarz H. L., Miller T. M., Bederson B.: *Phys. Rev. A* **1974**, *10*, 1131.
35. Jitrik O., Bunge C. F.: *Phys. Rev. A* **1991**, *43*, 5804.
36. Dykstra C. E., Schaefer III H. F., Meyer W.: *J. Chem. Phys.* **1976**, *65*, 5141.
37. Huber K. P., Herzberg G.: *Constants of Diatomic Molecules* (data prepared by J. W. Gallagher and R. D. Johnson III) in *NIST Chemistry WebBook, NIST Standard Reference Database*, No. 69 (W. G. Mallard and P. J. Linstrom, Eds). National Institute of Standards and Technology, Gaithersburg, MD 20899, U.S.A. November 1999 (http://webbook.nist.gov).
38. Nelson R. D., Jr., Lide D. R., Maryott A. A.: *Selected Values of Electric Dipole Moments for Molecules in the Gas Phase*. NSRDS-NBS10 1967.
39. Gaydon A. G.: *Dissociation Energies and Spectra of Diatomic Molecules*. Chapman and Hall Ltd., London 1968.
40. Stwalley W. C., Zemke W. T.: *J. Phys. Chem. Ref. Data* **1993**, *22*, 87.
41. Li X., Paldus J.: *J. Chem. Phys.* **2003**, *118*, 2470.
42. Partridge H., Langhoff S. R.: *J. Chem. Phys.* **1981**, *74*, 2361.

43. Boutalib A., Gadéa F. X.: *J. Chem. Phys.* **1992**, *97*, 1144.
44. Dulick M., Zhang K. Q., Guo B., Bernath P. F.: *J. Mol. Spectrosc.* **1998**, *188*, 14.
45. Mulliken R. S.: *Int. J. Quantum Chem., Quantum Chem. Symp.* **1971**, *5*, 95.
46. Li X., Paldus J.: *J. Chem. Phys.* **1995**, *102*, 2013; and references therein.